Bioorganic & Medicinal Chemistry 20 (2012) 7069–7082

Contents lists available at SciVerse ScienceDirect

Bioorganic & Medicinal Chemistry

journal homepage: www.elsevier.com/locate/bmc

Optimization and structure–activity relationships of a series of potent inhibitors of methicillin-resistant *Staphylococcus aureus* (MRSA) pyruvate kinase as novel antimicrobial agents

Nag S. Kumar [a], Emily A. Amandoron [b], Artem Cherkasov [b,c], B. Brett Finlay [d,e], Huansheng Gong [b], Linda Jackson [e], Sukhbir Kaur [b], Tian Lian [b], Anne Moreau [a,†], Christophe Labrière [a], Neil E. Reiner [b,e], Raymond H. See [b,f], Natalie C. Strynadka [d], Lisa Thorson [b], Edwin W. Y. Wong [a], Liam Worrall [d], Roya Zoraghi [b], Robert N. Young [a,*]

[a] *Department of Chemistry, Simon Fraser University, Burnaby, Canada*
[b] *Department of Medicine, Division of Infectious Diseases, University of British Columbia, Vancouver, BC, Canada*
[c] *Vancouver Prostate Centre, Vancouver, BC, Canada*
[d] *Department of Biochemistry and Molecular Biology, University of British Columbia, Vancouver, BC, Canada*
[e] *Department of Microbiology and Immunology, Michael Smith Laboratories, University of British Columbia, Vancouver, BC, Canada*
[f] *University of British Columbia Centre for Disease Control, Vancouver, BC, Canada*

ARTICLE INFO

Article history:
Received 24 July 2012
Revised 25 September 2012
Accepted 3 October 2012
Available online 17 October 2012

Keywords:
Methicillin-resistant *Staphylococcus aureus*
Antimicrobial
Pyruvate kinase inhibitor
Structure–activity relationships

ABSTRACT

A novel series of hydrazones were synthesized and evaluated as inhibitors of methicillin-resistant *Staphylococcus aureus* (MRSA) pyruvate kinase (PK). PK has been identified as one of the most highly connected 'hub proteins' in MRSA. PK has been shown to be critical for bacterial survival which makes it a potential target for development of novel antibiotics and the high degree of connectivity implies it should be very sensitive to mutations and thus less able to develop resistance. PK is not unique to bacteria and thus a critical requirement for such a PK inhibitor would be that it does not inhibit the homologous human enzyme(s) at therapeutic concentrations. Several MRSA PK inhibitors (including **8d**) were identified using in silico screening combined with enzyme assays and were found to be selective for bacterial enzyme compared to four human PK isoforms (M1, M2, R and L). However these lead compounds did not show significant inhibitory activity for MRSA growth presumably due to poor bacterial cell penetration. Structure–activity relationship (SAR) studies were carried out on **8d** and led us to discover more potent compounds with enzyme inhibiting activities in the low nanomolar range and some were found to effectively inhibit bacteria growth in culture with minimum inhibitory concentrations (MIC) as low as 1 μg/mL. These inhibitors bind in two elongated flat clefts found at the minor interfaces in the homo-tetrameric enzyme complex and the observed SAR is in keeping with the size and electronic constraints of these binding sites. Access to the corresponding sites in the human enzyme is blocked.

1. Introduction

The rapid increase in antibiotic-resistant hospital-borne infections such as methicillin-resistant *Staphylococcus aureus* (MRSA) and vancomycin-resistant *Staphylococcus aureus* (VRSA) is creating a crisis in public health systems in the developed world. Recently, these infections have begun to find their ways out into the general community and this growing phenomenon only offers to worsen the crisis. Little progress has been made in the past several decades to identify new antibacterial targets that could be less prone to the development of resistance. A general principle of antibiotic target selection has been to target critical proteins and processes unique to the bacteria and without human homologs so as to avoid mechanism-based toxicity. This has severely limited the target options.

We have recently described preliminary results of an alternative effort wherein a highly interconnected 'hub protein', bacterial pyruvate kinase (PK), was selected for evaluation[1] based on considerations that; (1) the essentiality of the enzyme should render inhibition lethal, (2) the high connectivity should confound the

Abbreviations: MRSA, methicillin-resistant *Staphylococcus aureus*; PK, pyruvate kinase; MIC, minimal inhibitory concentration; VRSA, vancomycin-resistant *Staphylococcus aureus*.

* Corresponding author. Tel.: +1 778 782 3351; fax: +1 778 782 3765.
E-mail addresses: roberty@sfu.ca, robert_young@sfu.ca (R.N. Young).
† Current address: 186 bis, Avenue du Marechal Joffre, 1 Villa Leseur, 94170 Le Perreux-sur-Marne, France.

0968-0896/$ - see front matter © 2012 Elsevier Ltd. All rights reserved.
http://dx.doi.org/10.1016/j.bmc.2012.10.002

viability of mutations that might seek to produce resistant strains, (3) there is no known available 'escape' paralog enzyme in the bacterial genome, (4) there is a wealth of available structural information on both the bacterial and human homologous enzymes and (5) there are unique peptide sequence insertion and deletion differences between the bacterial and human enzymes that appear to produce druggable lipophylic pockets on the bacterial enzyme that are absent on the human forms. One of these pockets was probed in an in silico screening effort[2] which led to the identification of a number of compounds with MRSA PK inhibiting activities in the low nanomolar range (e.g. **IS-63**) that were selective over the four known human homologs (M1, M2, R and L). A subsequent round of similarity searching and screening identified compound **IS-130** (**8d**) (Fig. 1) that was 10-fold more potent (IC_{50} 91 nM) and selective (>1000-fold) over the human PK. However, neither compound showed efficacy in inhibiting growth of intact bacteria suggesting that they were unable to pass through the bacterial cell wall (see Table 1). Subsequent exploration of structure–activity relationships and optimization of physico-chemical properties identified analogs (such as compounds **7d** and **6ϕ**) which were both potent enzyme inhibitors and which showed effective inhibition of a wide panel of gram positive bacterial growth comparable to standard antibiotics such as vancomycin.[3] We eventually were able to obtain an X-ray structure for **8d** and **6ϕ** bound to MRSA282 PK which revealed that the compounds do not bind to the originally targeted lipophilic pocket but rather in a flat lipophilic pocket at the minor interfaces in the homo-tetrameric enzyme structure (see Fig. 2).[2] Subsequently some dimeric indole natural products have also been shown to bind to the same site.[4] Differing sequences for the bacterial versus human enzymes meant that this binding site was not accessible in the human PK enzymes (see Discussion). PK is thought to be significantly more active in its tetrameric form and it is not entirely clear how this binding inhibits activity. It has been hypothesized that allosteric binding at this site may prevent the enzyme tetramer from adopting a more compressed and rigidized confirmation required for effective enzymatic activity.[4] Notably, MRSA passaged 25 consecutive times in the presence of sub-lethal concentration of **7d** did not develop significant resistance suggesting that inhibition of MRSA PK may indeed yield anti-bacterial agents that are less prone to develop any resistance.[3]

In this paper we present a detailed account of structure–activity relationships for enzyme inhibitory and optimization of antibacterial activity for an extensive series of indole hydrazones.

Table 1
PK inhibitory activity and antimicrobial activity of compounds with modification on the indole moiety

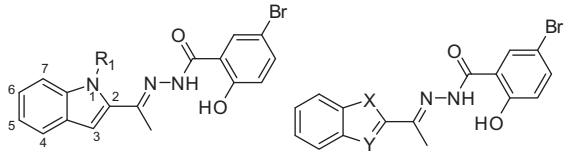

6a-n,7a-j **8a-d**

Analogues	IC_{50} (nM)[a]	MIC[b] (μg/mL)	R_1	Substitutions
6a	85 (2)	>186	H	
6b	49 (2)	>195 (2)	H	5-Fluoro
6c	52 (2)	>81(2)	H	5-Chloro
6d	49 (3)	>226	H	5-Bromo
6e	43 (2)	>64 (2)	H	5-Iodo
6f	46% @ 10 μM	ND	H	5-Trifluoromethyl
6g	214	*>64	H	5-Hydroxy
6h	178 (2)	>80	H	5-Methoxy
6i	0% @ 1 μM	>90	H	5-Phenyl
6j	24	*>64	H	6-Bromo
6k	20	>82	H	5,6-Difluoro
6l	24 (2)	41	H	4,5-Difluro
6m	39% @ 0.5 μM	>156	H	7-Fluoro
6n	15	**>85	H	4,5,6-Trifluoro
7a	381 (2)	**7.7 (3)	CH_3	
7b	165 (2)	3.3 (3)	CH_3	5-Fluoro
7c	228	1.3 (5)	CH_3	5-Chloro
7d	146 (3)	1.4 (2)	CH_3	5-Bromo
7e	54% @ 1 μM	*>64	CH_3	5-Hydroxy
7f	794	10.4	CH_3	5-Methoxy
7g	17	1.0	CH_3	6-Bromo
7h	61	1.6 (2)	CH_3	5,6-Difluoro
7i	145 (2)	2.0 (2)	CH_3	4,5-Difluoro
7j	55	**2.0	CH_3	4,5,6-Trifluoro
8a	286 (2)	>195	—	X = S, Y = CH
8b	224	>78 (3)	—	X = S, Y = N
8c	26% @ 0.5 μM	**>150	—	X = O, Y = N
8d	91 (2)	>187	—	X = NH, Y = N
8e	227	>194(2)	—	X = NCH_3, Y = N

[a] IC_{50} values are calculated from triplicate 15 point titrations or are an average of (*n*) such determinations as indicated. Alternatively the % inhibition at the highest concentration tested is presented.

[b] Minimum concentration to give >98% inhibition of growth of *S. aureus RN4220*, **S. aureus ATCC 25923 or* ***ATCC 29213* (single determination or average of (n) determinations). Control MIC (vancomycin) is 1 μg/ml.

2. Results

2.1. Chemistry

The syntheses of all target compounds were carried out as described in Schemes 1 through 4. Palladium-catalyzed annulation of *ortho*-iodoanilines and 2-oxopropanoic acid gave 2-carboxylic acid indoles (**1**) (Scheme 1). Treatment of **1** with MeLi furnished the methyl ketones (**3a–f**). In the case where R_5 is ethyl, *t*-butyl or phenyl, the 2-carboxylic acid indole (**1**) was first converted to Weinreb amide (**2**) (in order to avoid double addition) which was subsequently treated with either Grignard or organolithium reagent to give ketones **3l–n**. To make the aldehyde derivatives (R_5 is H), compound **1** was reduced to an alcohol with $LiAlH_4$ and then re-oxidized with MnO_2 to give aldehyde **3o**. Subsequently, compound **3** was coupled to the hydrazide **5** (which was prepared from the corresponding ester and hydrazine) by a simple condensation reaction either in neutral or mild acidic conditions to give compound **6**. In order to prepare compound **7**, intermediate **3** was first alkylated with alkyl halide and then condensed with hydrazide **5**. Compounds **8** and **10** were prepared in a similar manner where an appropriate ketone was condensed with phenyl, pyridine or naphthalene hydrazides (Scheme 2).

N-methyl hydrazide **9** was synthesized from 1-(1*H*-indol-2-yl)ethanone (**3p**) where it was first treated with methylhydrazine to form a Schiff's base and subsequently reacted with an activated salicylic acid derivative to give compound **9** (Scheme 3). Compound **12** with an oxime linking moiety was synthesized by reacting appropriate acid chloride with oxime **11**, which was itself prepared from the corresponding ketone **3** by condensation with hydroxylamine hydrochloride in presence of pyridine. Finally the sulfonohydrazide **13** was made by coupling appropriate methyl ketone with 5-bromo-2-methoxybenzenesulphonohydrazide which

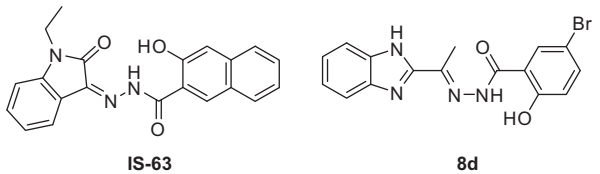

Figure 1. MRSA PK inhibitors identified through in silico screening.

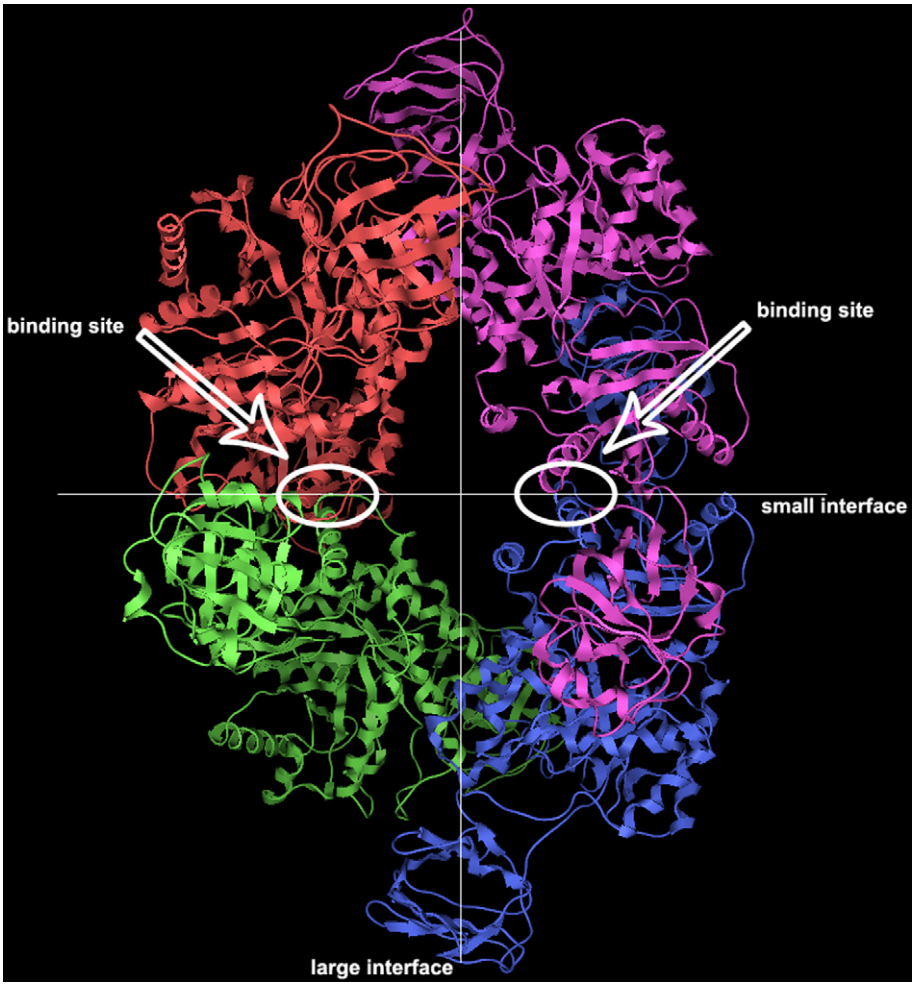

Figure 2. Resolved structure of MRSA252 pyruvate kinase tetramer showing the domain boundaries and tetramer architecture. Each monomer has been coloured to facilitate the identification of the small and large interface shown as lines. The binding site located at the small interface sits in between two alpha helices formed by two PK monomers shown as circles.

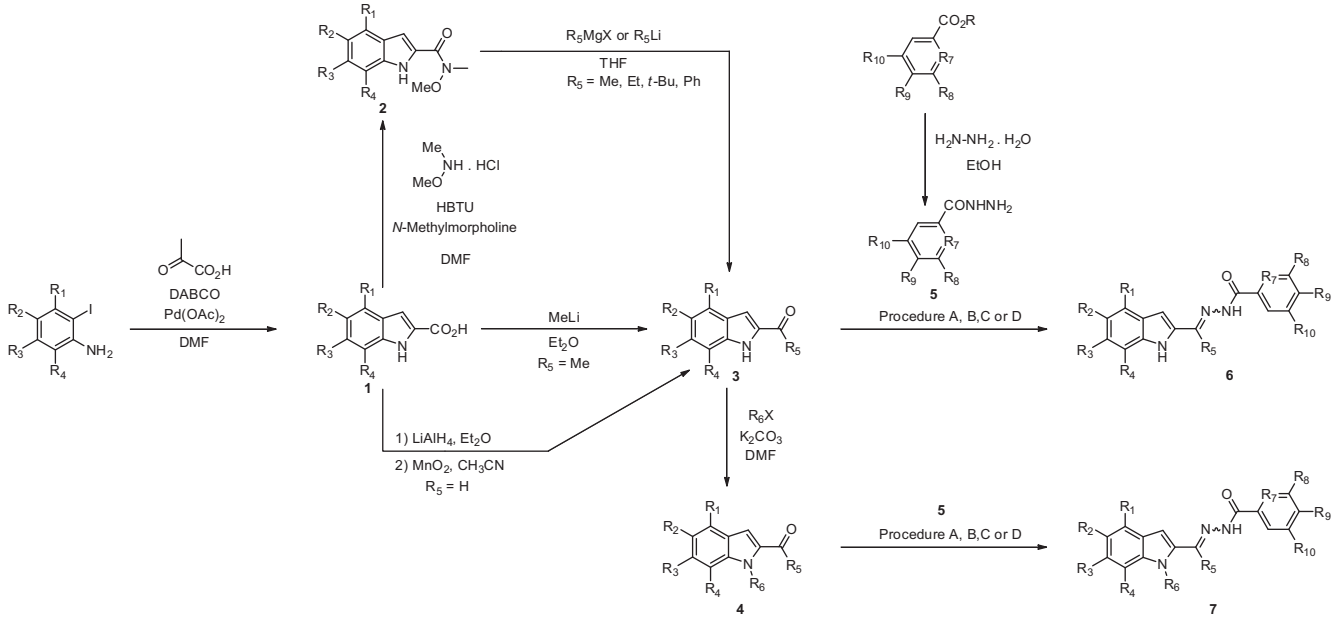

Scheme 1. General syntheses of the hydrazones **6** and **7**. Procedure: (A) nPrOH, reflux. (B) EtOH, reflux. (C) AcOH, nPrOH, reflux. (D) AcOH, EtOH, reflux.

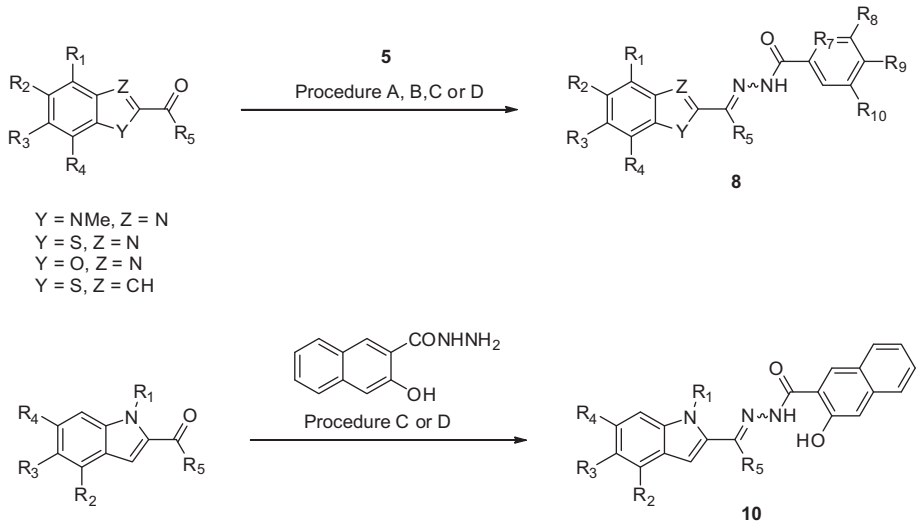

Scheme 2. Preparation of hydrazones **8** and **10**. Procedure: (A) nPrOH, reflux. (B) EtOH, reflux. (C) AcOH, nPrOH, reflux. (D) AcOH, EtOH, reflux. (E) EtOH, MW at 100 °C.

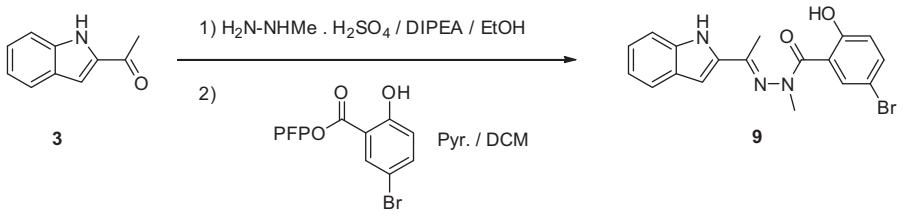

Scheme 3. Preparation of *N*-methyl hydrazones **9**.

was prepared by condensing 5-bromo-2-methoxyphenyl-1-sulfonyl chloride with hydrazine (Scheme 4).

2.2. Biological results and SAR studies

Compounds were evaluated to determine their ability to inhibit MRSA pyruvate kinase (PK) activity and for selected compounds selectivity was determined using the mammalian PK isoforms M1, M2, R and L. Of those compounds tested for selectivity none showed inhibition of the mammalian PK isoforms greater than 50% and they generally showed no significant inhibition (<20%) at the highest concentration tested (10 μM) (See Tables 6–9 Supplementary data). Cellular antimicrobial activity was evaluated for ability to fully inhibit the growth of MRSA in culture (determining minimum inhibitory concentration (MIC) values). Cytotoxicity was evaluated for selected compounds using mammalian cells (THP-1 or Hela 293).

2.2.1. SAR for in vitro inhibition of MRSA PK

The lead structure **8d** showed interesting potency on the MRSA PK enzyme but not in the cellular anti-MRSA assay and so we set out to develop SAR for both enzyme inhibition and antibacterial

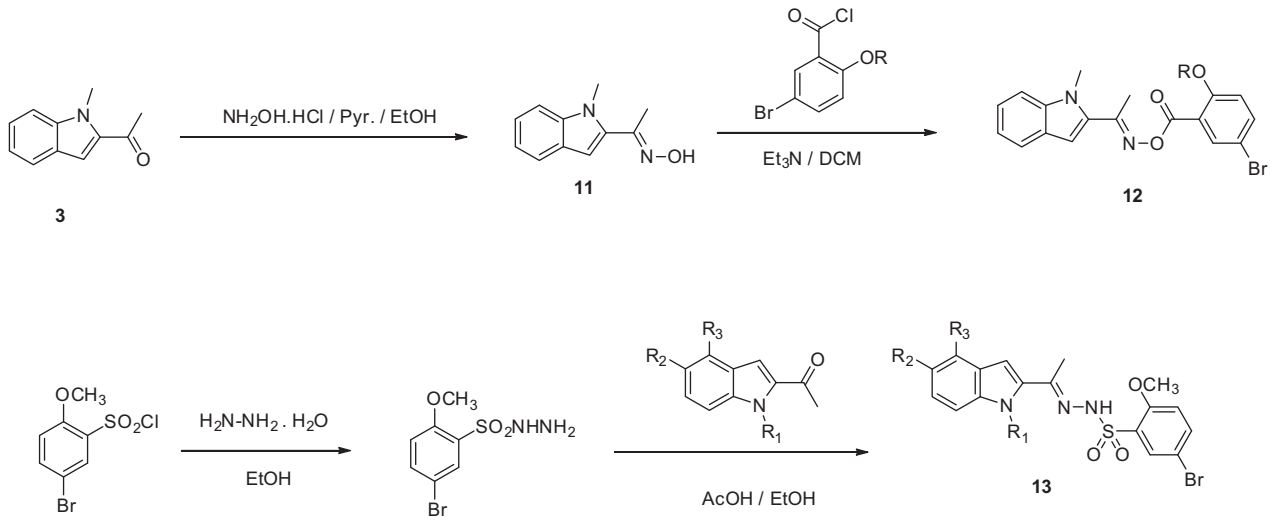

Scheme 4. Preparation of oxime linker 12 and sulfonohydrazide linker 13.

Table 2
PK inhibitory activity and antimicrobial activity of phenol modified derivatives

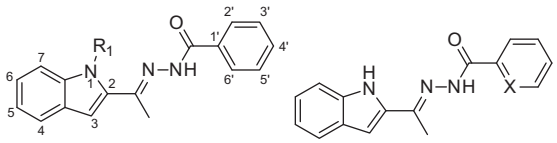

6s

Analogues	IC_{50} (nM)[a]	MIC[b] (μg/mL)	R_1	Substitutions
6o	8150 (2)	>178	H	5′-Bromo
6p	8615	59 (3)	H	2′-Hydroxy
6q	1312	ND	H	2′-Hydroxy-4′-bromo
6r	28% @ 10 μM	>139	H	
6s	15% @ 10 μM	>139	—	X = N
6t	36% @ 1 μM	>64	H	2′-Hydroxy-5′-chloro
6u	151	>84 (2)	H	2′-Hydroxy-5′-iodo
6v	20% @ 10 μM	ND	H	2′-Hydroxy-5′-phenyl
6w	182	>193	H	2′-Methoxy-5′-bromo
6x	63	**>64	H	2′-Ethoxy-5′-bromo
6y	251	**>64	H	2′-Ethoxymethoxy-5-bromo
6z	64 (2)	>205	H	2′-(Prop-2-yn-1-yloxy)-5-bromo
6α	74	64	H	2′-Hydroxy-3′,5′-dibromo
6β	57% @ 1 μM	*>93	H	2′-Methoxy-3′,5′-dibromo
6χ	40% @ 10 uM	ND	H	2′-Hydroxy-3′,5′-diisopropyl
6δ	324	>161	H	2′-Hydroxy-4′-methoxy-5′-bromo
7k	483	5.4	CH_3	2′-Hydroxy-5′-iodo
7l	61% @ 0.5 μM	4.8	CH_3	2′-Hydroxy-4′-bromo
7m	841	>167	CH_3	2′-Hydroxy-4′-methoxy-5′-bromo

[a] IC_{50} values are calculated from triplicate 15 point titrations or are an average of (n) such determinations as indicated. Alternatively the % inhibition at the highest concentration tested is presented.

[b] Minimum concentration to give >98% inhibition of growth of *S. aureus RN4220* or **S. aureus ATCC 25923 or* ***ATCC 29213* (single determination or average of (n) determinations).

activity in parallel. However, for purpose of clarity we will discuss the SAR derived for the in vitro enzyme inhibition separately from the cellular antibacterial activity. We systematically evaluated structural changes in the three regions of the lead molecule (**8d**); the 'left hand' heteroaryl moiety (Table 1), the 'right hand' phenolic moiety (Tables 2 and 5) and central linking moiety (Tables 3 and 4)

To evaluate the role of the benzimidazole nitrogen functions in compound **8d** we prepared a series of heterocyclic analogs. Thus the corresponding indole (**6a**), benzothiophene (**8a**), benzothiazole (**8b**), and benzoxazole (**8c**) analogs were prepared and notably **6a** retained potency and selectivity (compared to **8d)** while **8a** and **8b** were about 3-fold less potent and **8c** was much less potent (Table 1). Similarly the *N*-methylated benzimidazole (**8e**) lost about 3-fold potency compared to **8d** and the *N*-methyl indole **7a**, was about 4-fold less active (than the parent **6a)** thus suggesting that neither a basic nitrogen nor an NH were critical of enzyme inhibitory activity. At this point, observation of anti-MRSA activity in the analog **7a** caused us to focus efforts on the indole series. We thus evaluated the effect of substitution(s) on the indole ring. Halogen substitution at positions 5 (compounds **6b–e**) or 6 (**6j**) led to 2 to 4-fold increased potency (relative to **6a**) as did multi-substitution at positions 4,5 (**6l**), positions 5,6 (**6k**) or 4,5,6 (**6n**). Notably, the 7-fluoro analog **6m** was much less potent suggesting this face of the molecule could not tolerate substitution. Equally, bulky substituents at position 5 (**6f** and **6i**) lost most or all activity. Polar substitutions such as OH or OCH_3 (**6g** or **6h**) were tolerated but trended to lesser potency.

We also investigated the effects of substitutions on the *N*-methyl indole series and found that (relative to **7a**), 5-halogen substituted compounds (**7b**, **7c** and **7d**) appeared to be slightly more potent while the 6-bromo analog **7g** was most potent (IC_{50} 17 nM). Polyhalogenated analogs (**7h**, **7i** and **7j**) showed either no advantage or lost potency. The 5-hydroxy (**7e**) or 5-methoxy (**7f**) analogs were much less potent.

We next turned our attentions to the phenolic element in these hydrazones (Table 2). Removal of either the hydroxyl- or bromo-substituents (or both) led to a dramatic drop in activity (**6o, 6p, 6r**) while placing the bromine at the 4′ position led to a less dramatic (ca. 10-fold) loss in activity. Notably, the phenolic hydroxyl function could not be replaced by a pyridine nitrogen (**6s**) nor could the 5′ bromine be replaced by chlorine (**6t**). However the corresponding iodo-analog (**6u**) had similar potency compared to **6a** suggesting these substituents occupied an important lipophilic binding pocket. Compound **6v**, with phenyl substitution at the 5′ position, was essentially inactive indicating that this pocket was of limited size. It was interesting to note that the hydroxyl function in **6a** could be substituted (**6w, 6x, 6y, 6z**) with little or no loss in activity, which strongly suggested that the oxygen in all these compounds was acting as a hydrogen bond acceptor and not a donor. Simple modelling energy calculations (MM2; ChemDraw) suggested that the hydrazone NH forms a strong hydrogen bond with these adjacent oxygen atoms and that this serves to flatten and orient the critical bromine atom in a specifically defined direction. Subsequently, X-ray diffraction of **6ϕ** (Fig. 3) as well as X-ray structural analysis on **8d**[2] and **6ϕ** (unpublished) bound to MRSA PK (Fig. 4) confirmed this orientation. We also prepared several analogs with multiple substitutions on the 'phenol' ring and found that the 3′,5′-dibromo analog (**6α**) was essentially equipotent when compared with **6a** while interestingly, the corresponding methoxy analog **6β** was less active when compared to its analogous monobromo analog **6w**. This likely reflects the steric compression that the methoxyl methyl experiences from the adjacent bromine atom as it tries to orient itself to achieve the important hydrogen bond with the hydrazone NH. A 3′,5′-diisopropyl analog **6χ** was not active while the 4′-methoxy-5′-bromo analog **6δ** showed reduced but still significant activity. 4′,5′-disubstitution was shown to be tolerated as reinforced by the potent enzyme inhibitory activity we observe for some naphthalene analogs (**10a**, **10b**; Table 5).

Our next step was to investigate the structural requirements for enzyme inhibitory activity as it related to the linking hydrazone element (Tables 3 and 4). Replacing the R_2 methyl group with hydrogen led to a loss of activity (**6ε**) while replacing it with an ethyl group (**6ϕ)** retained activity. The phenyl-substituted analog (**6φ**) showed a 4 to 5-fold loss of activity on the enzyme. Finally, the *t*-butyl analog **6ι** was prepared and found to be essentially inactive on the enzyme. NMR analysis and the X-ray diffraction structure (Fig. 3) indicated **6ι** was completely present as the *Z*-isomer and presumably this dramatic shape change is not accommodated by the enzyme binding site.

We next examined the NH and carbonyl functions of the linker element and found that the *N*-methyl hydrazone (**9**) and the acyloxylamines (**12a, 12b**) were essentially without activity. This is in keeping with the crucial role the NH plays via a hydrogen bond in orienting the phenol ring and the bromine atom. Notably the sulphonamides (**13a** and **13b**) were also inactive. This may relate to the need for absolute planarity in this part of the binding site.

2.2.2. Structural and molecular modelling studies

The SAR observations for inhibition of MRSA PK were found to agree very well with the binding site revealed in the X-ray

Table 3
PK inhibitory activity and antimicrobial activity of compounds with modification on the linker

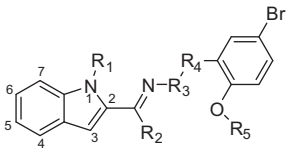

Analogues	IC_{50} (nM)[b]	MIC[c] (μg/mL)	R_1	R_2	R_3	R_4	R_5	Substitutions
6ε	863(3)	>179	H	H	NH	C(O)	H	
6ϕ	126 (2)	9.7	H	C_2H_5	NH	C(O)	H	
6γ	451	**>64	H	H	NH	C(O)	CH_3	
6η	49	**4.0	H	C_2H_5	NH	C(O)	H	5-Bromo
7n	168	**2.0	CH_3	C_2H_5	NH	C(O)	H	5-Bromo
7o	3087 (2)	>186	CH_3	H	NH	C(O)	H	
7p	461	5	CH_3	C_2H_5	NH	C(O)	H	
9[a]	33% @ 1 μM	*>80	H	CH_3	NCH_3	C(O)	CH_3	
12a	34% @ 10 μM	>155	CH_3	CH_3	O	C(O)	H	
12b	33% @ 10 μM	>161	CH_3	CH_3	O	C(O)	CH_3	
13a	12% @ 10 μM	ND	H	CH_3	NH	SO_2	CH_3	
13b	11% @ 10 μM	ND	H	CH_3	NH	SO_2	CH_3	4,5-Difluoro

[a] Present in two isomeric forms, major isomer shown.
[b] IC_{50} values are calculated from triplicate 15 point titrations or are an average of (*n*) such determinations as indicated. Alternatively the % inhibition at the highest concentration tested is presented.
[c] Minimum concentration to give >98% inhibition of growth of *S. aureus RN4220* or **S. aureus ATCC 25923 or* ***ATCC 29213* (single determination or average of (n) determinations).

Table 4
PK inhibitory activity antimicrobial activity and cytotoxicity in mammalian THP-1 cells for compounds which are either exclusively present in Z configuration (**6ι,7q**) or in two isomeric forms (**6φ**, **7r**)

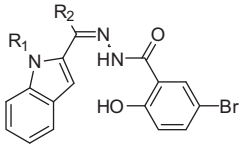

Analogues	IC_{50} (nM)[b]	MIC[c] (μg/mL)	R_1	R_2	Cytotoxicity (% dead THP-1 cells)	
					25 μM	6.25 μM
6ι	0% @ 10 μM	83	H	$C(CH_3)_3$	50	42
6φ[a]	445 (2)	1.4 (2)	H	Ph	83	43
7q	0% @10 μM	10.7	CH_3	$C(CH_3)_3$	73	25
7r[a]	6043	1.4	CH_3	Ph	78	19

[a] Present in two isomeric forms.
[b] IC_{50} values are calculated from a triplicate 15 point titration or are an average of (*n*) such determinations as indicated. Alternatively the % inhibition at the highest concentration tested is presented.
[c] Minimum concentration to give >98% inhibition of growth of *S. aureus RN4220* (single determination or average of (*n*) determinations).

structure obtained for compounds **8d**[2] and **6ϕ** (unpublished) bound to MRSA252 pyruvate kinase (Fig. 4). These two identical binding sites are located at the minor interface between the parallel domains of the enzyme tetramer (between monomers A and B and between monomers C and D). The pockets are flat and elongated and accessible in the MRSA PK but access in the human PK isoforms is blocked by five amino acids (Glu 418-B, Arg 399-A and B and Arg 400 A and B) (the corresponding amino acids in MRSA PK are His 365-B, Lys-349 A and B and Thr 348-A and B) (see Fig. 5). Despite the resolution of the data for the compounds in complex with MRSA PK (3.1 Å for **8d** and 3.3 Å for **6ϕ**), the agreement with the independently determined small molecule X-ray

Table 5
PK inhibitory activity and antimicrobial activity of naphthol derivatives

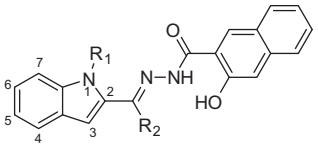

Analogues	IC_{50} (nM)[a]	MIC (μg/mL)[b]	R_1	R_2	Substitutions
10a	42	>64	H	CH_3	
10b	26	>64	H	CH_3	5-Bromo
10c	31	>64	H	C_2H_5	4,5,6-Trifluoro
10d	18	16	H	C_2H_5	5-Bromo
10e	115	>64	CH_3	CH_3	5-Bromo
10f	79	1	CH_3	C_2H_5	5-Bromo
10g	59	>64	CH_3	CH_3	4,5,6-Trifluoro
10h	52	32	CH_3	C_2H_5	4,5,6-Trifluoro

[a] IC_{50} values are calculated from a triplicate 15 point titration unless otherwise noted.
[b] Minimum concentration to give >98% inhibition of growth of *S. aureus ATCC 29213* (single determination unless noted).

structure of **6ϕ** gives us confidence in the modelled orientation in the interface binding pocket. The ligand in the X-ray structure was found to exist in the expected conformation with a hydrogen bond between the hydrazone NH and the phenol oxygen. The 5-bromo substituent was oriented toward the interior of the site in a deep lipophilic pocket formed by Ala 358-A and Ile 351-A. The indole NH, hydrazone C=N and carbonyl all appear to form hydrogen bonds to serine 362-A and B which is also interior to the site (see Fig. 4). The phenol and ethyl group of **6ϕ** are oriented towards the outside (water side) of the binding site in keeping with our observations that the phenol could be substituted with a variety of short or long chains without significant loss of activity. Equally we observed that the ethyl group can be replaced by a flat phenyl group but not with the bulky *t*-butyl group that disfavours the elongated E-isomer. The X-ray structure revealed some vacant space in the vicinity of the indole phenyl ring to allow for small substitution but indicated a tight fit adjacent to the indole NH (the 7-position) that would be in keeping with the observed intolerance for substitution at that position. It is not clear if the methyl group of the *N*-methyl indole analogs can be accommodated oriented to the interior or would prefer the exterior of the site. The former appears to also be a tight fit but may nonetheless be preferred as the 'outside' rotamer would produce a *peri* interaction between the ethyl group (or methyl) of the hydrazone and the *N*-methyl of the indole and thus it seems unlikely that strict planarity could be maintained. Perhaps the tolerability of non-planarity is greater in this part of the binding site. Nonetheless, *N*-methylation would remove the putative H-bond between the indole NH and serines 362 (vide supra) and thus would explain the 3 to 4-fold loss of potency for the *N*-methyl versus the NH indole compound pairs.

2.2.3. SAR for anti-MRSA activity

In spite of the relatively potent MRSA PK inhibitory activity observed of the original benzimidazole lead (**8d**) and the analogous benzoheterocycles (**6a, 8a, 8b, 8d**) these compounds did not show significant anti-MRSA activity at concentrations 300 to 1000-fold higher than enzyme IC_{50}s (Table 1). Equally none of the series of substituted NH-indoles tested showed measureable MIC values with the exception of **6ϕ** and **6η** (Table 3) which gave MIC values of 9.7 and 4 μg/ml respectively.

Considering that the anti-MRSA activity of these compounds might be attributed to the added lipophilicity of the ethyl or the methyl group (*C*Log*P* values of 4.73 for **6ϕ** and 4.67 for **7a** versus 4.20 for **6a**) we investigated the *N*-methylated analogs in the indole series which were predicted to be more lipophilic than their

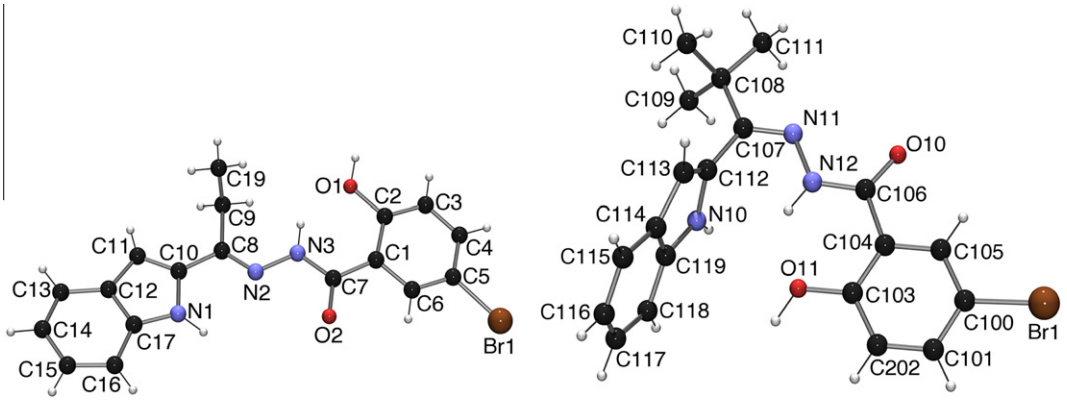

Figure 3. X-ray crystal structure diagrams of **6ϕ** (left) and **6ι** (right).

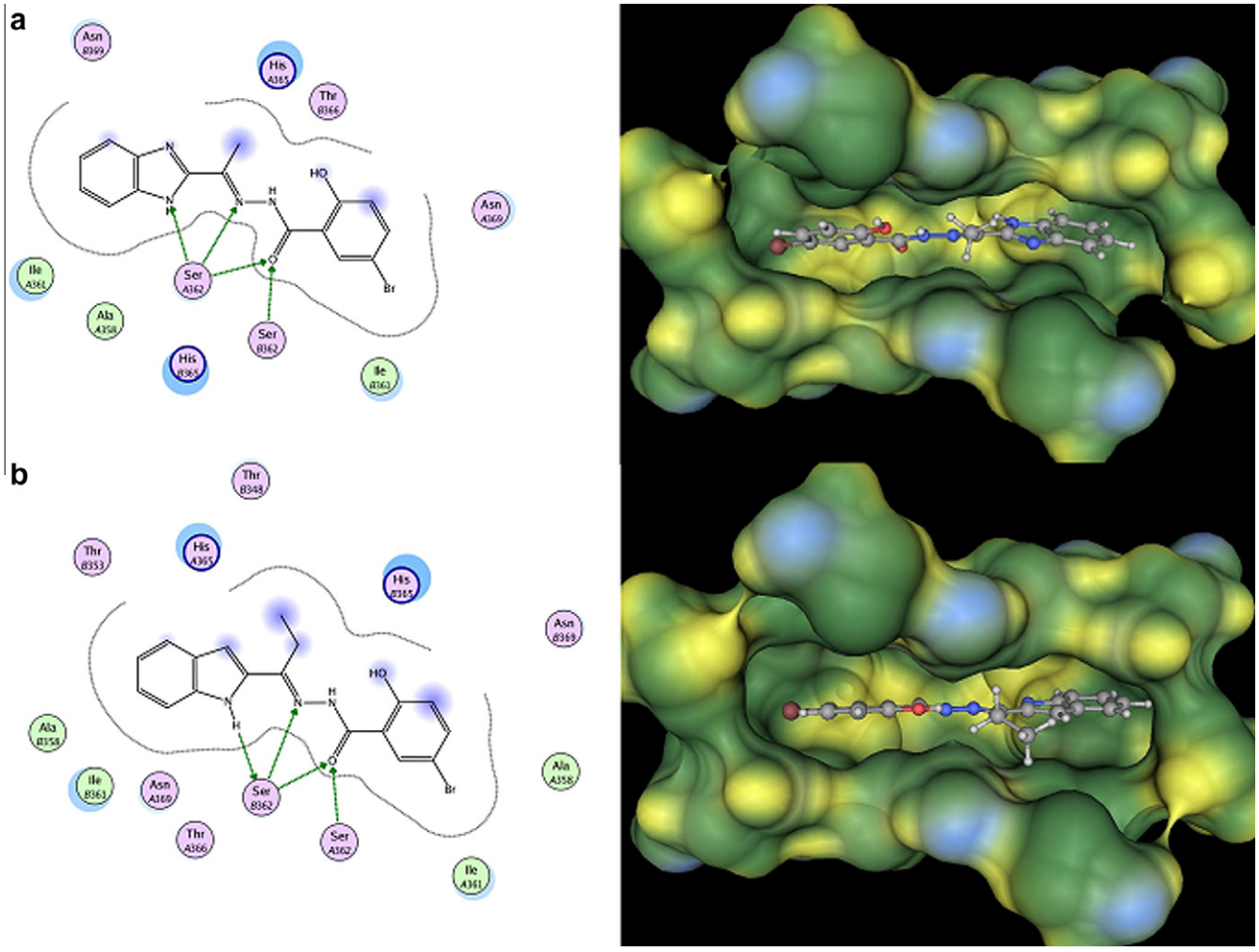

Figure 4. Binding mode of compounds **8d** and **6ϕ** at the interface binding site (a) a two-dimensional map of the binding interactions between **8d** and the interface site based on its co-crystallization with MRSA PK. Green arrows depict hydrogen-accepting interactions between **8d** and MRSA PK residues from the interface (left). Binding orientation of **8d** within the interface-binding pocket based on the protein–ligand crystal structure (right). (b) The same view for **6ϕ**.

NH counterparts (Table 10, Supplementary data). We were gratified to observe that many of these *N*-methylated analogs gave good to excellent MIC values (see Table 1). Although the CLogP values for *N*-methyl indole derivatives (**7a–j**) were calculated to be generally 0.3–0.6 higher than the corresponding NH derivatives, in an absolute sense there was no clear correlation of *C*Log*P* and MIC. In addition, we noted that while the *N*-methyl indole analogs (**7k**, **7l**) showed reasonable MICs, surprisingly, the corresponding naphthalene analogs, **10e** and **10g**, did not (although the naphthalene analog with R_2 = ethyl (**10f**) had an excellent MIC of 1 μg/ml (Table 5). Thus it was apparent that the SAR for antibacterial activity was not fully transferable from the phenyl to the naphthalene series and in general the factors affecting translation of in vitro enzyme inhibition potency to anti-MRSA activity are unclear.

While characterizing the compounds we noted that while the NH indoles or benzimidazoles exist as one isomer at room temperature (as evidenced in their NMR spectra), the N-methyl analogs showed evidence of variable ratio of isomers[5] which interconverted rapidly at higher temperature. It is assumed these isomers are rotamers about the 2-indole C–C bond. What effect this phenomenon may have on the anti-MRSA activity is also unclear.

In investigating the effects of substitutions in the hydrazone linking moiety we noted that some compounds (**6ι**, **6φ**, **7q**, **7r**) with bulky groups on the bridging hydrazone showed good MIC values in the cell assay in spite of very weak potency as inhibitors of MRSA PK (Table 4). This lack of correlation was surprising but notably 6φ was found (NMR and HPLC) to exist in two isomeric forms about the hydrazone double bond (although the *E*-isomer predominated) and, as noted above, the corresponding *t*-butyl analog **6ι** was found by X-ray analysis to exist exclusively as the *Z*-isomer.

These 'anomalous' antibacterial activities suggested that these isomeric compounds may exert antibacterial activity via a different (unknown) mechanism and, as these compounds show significant or predominant propensity to exist in the *Z*-configuration, this off-target activity may relate to the *Z*-isomer rather than the *E*-isomer. Notably these 'anomalous' compounds (**6ι. 6φ 7q**, **7r**), also showed significant cytotoxicity on mammalian THP-1 cells with LD_{50}s between 6–25 μg/ml while comparable compounds (e.g. **7a**, **7b**, **7d**) that existed as predominantly *E*-isomers did not show mammalian cell cytotoxicity at much higher concentrations (LD_{50} >500 μg/ml) (Table 4 and data not shown).

3. Conclusion

In summary, a series of potent inhibitors of MRSA PK were synthesized in order to understand the SAR and to further optimize the physiochemical properties for effective inhibition of bacterial growth in vitro and, potentially, in vivo. X-ray structures for compounds **8d** and **6ϕ** bound to MRSA252 PK show that the active compounds fit in a very flat and elongated binding site with an important interior lipophilic binding pocket which is best fit by an appropriately appended and oriented bromine atom or naphthalene equivalent. The pre-organization and flat structure enforced by suitably placed hydrogen bonds is also very important. Correlation of in vitro enzyme inhibitory activity and anti-MRSA activity was poor although some compounds, generally N-methyl indole analogs, showed excellent MIC values and lack of mammalian cytotoxicity. The lead compounds with best MIC values are currently being formulated and evaluated to maximize in vivo exposure in preparation for evaluation in in vivo animal infection models. These studies will be reported elsewhere.

4. Experimental Section

4.1. Chemistry

4.1.1. General synthesis methods

^{1}H and ^{13}C NMR spectra were recorded with either Bruker Avance II™ 600 MHz, Bruker Avance III™ 500 MHz or Bruker Avance III™ 400 MHz. Processing of the spectra was performed with MestRec™ software. The high-resolution mass spectra were recorded in positive ion-mode with an ESI ion source on an Agilent™ Time-of-Flight LC/MS mass spectrometer. Analytical thin-layer chromatography (TLC) was performed on aluminum plates pre-coated with silica gel 60F-254 as the absorbent. The developed plates were air-dried, exposed to UV light and/or dipped in $KMnO_4$ solution and heated. Column chromatography was performed with silica gel 60 (230–400 mesh). Purity of >95% for all final compounds was confirmed by analytical reverse-phase HPLC utilizing a Dikma Technologies™ Inspire® C18 reverse-phase analytical column (4.6 × 150 mm). All HPLC purifications were carried out using an Agilent™ C18 reverse-phase preparatory column (21.2 × 250 mm).

The syntheses of all the intermediates (**1**, **3**, **4**, **5, 11**) and *N*-acylhydrazones (**7, 8, 9, 10, 12, 13**) are described in detail in Supplementary data.

4.1.1.1. General procedures for the synthesis of the *N*-acylhydrazones 6–8. *Procedure A:* A mixture of the appropriate ketone (0.25 mmol) and hydrazide (0.25 mmol) in propan-1-ol (3 mL) was refluxed until completion (or good conversion) of the reaction (monitored by TLC). If the product precipitated, it was collected by filtration and the solid was washed with hot propan-1-ol

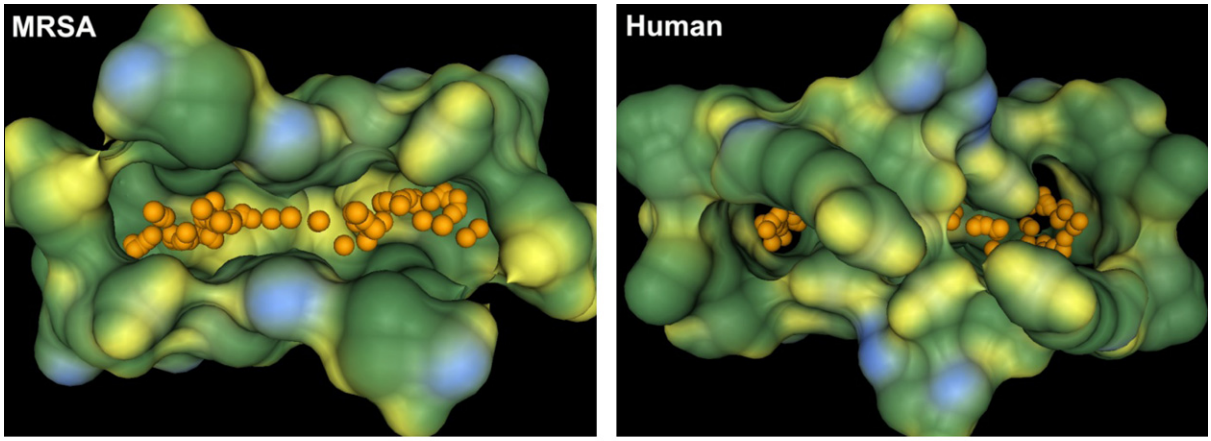

Figure 5. (a) Structures of the interface-binding site for MRSA and human PK. Orange spheres show the interface cavity in MRSA and human. The MRSA PK model shows an accessible binding pocket located at the interface of two PK monomers. In contrast, the pocket in human PK is partially obstructed by five amino acid residues (Glu418-B, Arg399-A, B and Arg400-A, B. (b) A sequence alignment showing the interface region (highlighted residues) for pyruvate kinase (PK) from *Staphylococcus aureus* and *homo sapiens*. The poorly conserved residues between MRSA and human PK are highlighted purple. The small interface also encompasses an insertion region in human PK (shown in yellow) and the corresponding deletion area in MRSA PK.

(10 mL). If no precipitation was observed, the solvent was evaporated in vacuo and the compound was purified by flash column chromatography.

Procedure B: A mixture of the appropriate ketone (0.35 mmol) and hydrazide (0.35 mmol) in EtOH (5 mL) was refluxed until completion (or good conversion) of the reaction (monitored by TLC). If the product precipitated, it was collected by filtration and the solid was washed with hot EtOH (2 × 2 mL). If no precipitation was observed, the solvent was evaporated in vacuo and the compound was purified by flash column chromatography.

Procedure C: A mixture of the appropriate ketone (0.41 mmol), hydrazide (0.41 mmol) and AcOH (1 drop) in propan-1-ol (4 mL) was refluxed until completion (or good conversion) of the reaction (monitored by TLC). If the product precipitated, it was collected by filtration and the solid was washed with hot propan-1-ol (2 × 2 mL). If no precipitation was observed, the solvent was evaporated in vacuo and the compound was purified either by flash column chromatography or by reverse-phase HPLC.

Procedure D: A mixture of the appropriate ketone (0.41 mmol), hydrazide (0.41 mmol) and AcOH (1 drop) in ethanol (4 mL) was refluxed until completion (or good conversion) of the reaction (monitored by TLC). If the product precipitated, it was collected by filtration and the solid was washed with hot ethanol (2 × 2 mL). If no precipitation was observed, the solvent was evaporated in vacuo and the compound was purified by flash column chromatography.

Procedure E: A mixture of the appropriate ester (1.0 equiv) and hydrazine hydrate (>3.0 equiv) in ethanol was irradiated with microwaves for 60 min at 100 °C. If the hydrazide precipitated, it was collected by filtration. If no precipitation was observed, the mixture was partitioned between ethyl acetate and water, the organic layer dried over Na_2SO_4 and evaporated in vacuo. To the hydrazide taken up in ethanol was added the appropriate ketone and AcOH (1 drop). The mixture was refluxed—classical heating—until completion (or good conversion) of the reaction (monitored by TLC). If the product precipitated, it was collected by filtration and the solid was washed with hot ethanol (2 × 2 mL). If no precipitation was observed, the solvent was evaporated in vacuo and the compound was purified by flash column chromatography.

4.1.1.2. (*E*)-*N*′-(1-(1*H*-indol-2-yl)ethylidene)-5-bromo-2-hydroxybenzohydrazide (6a). Compound **6a** was prepared from 1-(1*H*-indol-2-yl)ethanone (**3p**) and 5-bromo-2-hydroxybenzohydrazide (**5c**) using general **Procedure B**.

Yield = 53% (after flash chromatography 20/1; DCM/MeOH), pale yellow solid. Mp = 276–279 °C. ^{1}H NMR (600 MHz, DMSO-d_6): δ 12.12 (s, 1H), 11.31 (s, 2H), 8.09 (s, 1H), 7.59 (d, J = 8.7 Hz, 1H), 7.56 (d, J = 7.9 Hz, 1H), 7.49 (d, J = 8.2 Hz, 1H), 7.14 (t, J = 7.9 Hz, 1H), 7.01 (d, J = 7.8 Hz, 1H), 7.00 (t, J = 7.4 Hz, 1H), 6.98 (s, 1H), 2.38 (s, 3H). ^{13}C NMR (150 MHz, DMSO-d_6): δ 160.3, 155.7, 147.3, 137.7, 135.74, 135.65, 132.5, 127.6, 123.2, 120.7, 120.3, 119.33, 119.31, 112.1, 110.8, 104.9, 13.8. HRMS calcd for $(C_{17}H_{14}{}^{79}BrN_3O_2+H)^+$ 372.0342, found 372.0333.

4.1.1.3. (*E*)-5-Bromo-*N*′-(1-(5-fluoro-1*H*-indol-2-yl)ethylidene)-2-hydroxybenzohydrazide (6b). Compound **6b** was prepared from 1-(5-fluoro-1*H*-indol-2-yl)ethanone (**3a**) and **5c** using general **Procedure A**.

Yield = 46% (filtration), white powder. Mp = 262–263 °C. ^{1}H NMR (400 MHz, DMSO-d_6): δ 12.11 (br s, 1H), 11.42 (s, 1H), 11.32 (s, 1H), 8.09 (d, J = 2.4 Hz, 1H), 7.59 (dd, J = 8.6 Hz, 2.6 Hz, 1H), 7.48 (dd, J = 8.8 Hz, 4.8 Hz, 1H), 7.32 (dd, J = 10.0 Hz, 2.4 Hz, 1H), 7.03–6.96 (m, 3H), 2.37 (s, 3H). ^{13}C NMR (100 MHz, DMSO-d_6): δ 160.3, 157.0 (d, J = 230 Hz), 155.7, 147.0, 137.5, 135.7, 134.4, 132.5, 127.6 (d, J = 10 Hz), 120.3, 119.3, 113.2 (d, J = 9 Hz), 111.5 (d, J = 26 Hz), 110.8, 104.9 (d, J = 23 Hz), 104.6 (d, J = 5 Hz), 13.7. HRMS calcd for $(C_{17}H_{13}{}^{79}BrFN_3O_2+H)^+$ 390.0248, found 390.0247.

4.1.1.4. (*E*)-5-Bromo-*N*′-(1-(5-chloro-1*H*-indol-2-yl)ethylidene)-2-hydroxybenzohydrazide (6c). Compound **6c** was prepared from 1-(5-chloro-1*H*-indol-2-yl)ethanone (**3q**) and **5c** using general **Procedure C**.

Yield = 77% (filtration), pale yellow solid. Mp = 282–285 °C. ^{1}H NMR (600 MHz, DMSO-d_6): δ 12.11 (s, 1H), 11.52 (s, 1H), 11.34 (s, 1H), 8.09 (d, J = 2.6 Hz, 1H), 7.61 (d, J = 2.2 Hz, 1H), 7.60 (dd, J = 2.7 Hz, 8.7 Hz, 1H), 7.49 (d, J = 8.7 Hz, 1H), 7.15 (dd, J = 2.1 Hz, 8.7 Hz, 1H), 6.98 (d, J = 8.7 Hz, 1H), 6.96 (d, J = 1.5 Hz, 1H), 2.37 (s, 3H). ^{13}C NMR (150 MHz, DMSO-d_6): δ 160.8, 156.1, 147.3, 137.8, 136.6, 136.2, 133.1, 129.1, 124.3, 123.6, 120.8, 120.2, 119.8, 114.2, 111.3, 104.7, 14.2. HRMS calcd for $(C_{17}H_{13}{}^{81}BrClN_3O_2+H)^+$ 407.9931, found 407.9931.

4.1.1.5. (*E*)-5-Bromo-*N*′-(1-(5-bromo-1*H*-indol-2-yl)ethylidene)-2-hydroxybenzohydrazide (6d). Compound **6d** was prepared from 1-(5-bromo-1*H*-indol-2-yl)ethanone (**3r**) and **5c** using general **Procedure A.**

Yield = 61% (filtration), pale yellow solid. Mp = 295–299 °C. ^{1}H NMR (600 MHz, DMSO-d_6): δ 12.12 (br s, 1H), 11.53 (s, 1H), 11.35 (br s, 1H), 8.08 (d, J = 2.6 Hz, 1H), 7.75 (d, J = 1.8 Hz, 1H), 7.59 (dd, J = 2.6 Hz, 8.7 Hz, 1H), 7.45 (d, J = 8.7 Hz, 1H), 7.26 (dd, J = 1.9 Hz, 8.6 Hz, 1H), 7.02 (d, J = 8.7 Hz, 1H), 6.96 (d, J = 1.5 Hz, 1H), 2.37 (s, 3H). ^{13}C NMR (150 MHz, DMSO-d_6): δ 161.2, 156.6, 147.6, 138.1, 137.3, 136.6, 133.5, 130.3, 126.5, 123.7, 121.2, 120.3, 115.1, 112.7, 111.7, 105.0, 14.7. HRMS calcd for $(C_{17}H_{13}{}^{79}Br_2N_3O_2+H)^+$ 451.9428, found 451.9428.

4.1.1.6. 5-Bromo-2-hydroxy-*N*′-[(1*E*)-1-(5-iodo-1*H*-indol-2-yl)ethylidene]benzohydrazide (6e). Compound **6e** was prepared from 1-(5-iodo-1*H*-indol-2-yl)ethanone (**3m**) and **5c** using general **Procedure D.**

Yield: 64%, light brown solid. Mp = 272–274 °C. ^{1}H NMR (500 MHz, DMSO-d_6): δ 12.12 (s, 1H), 11.52 (s, 1H), 11.37 (s, 1H), 8.09 (d, J = 2.5 Hz, 1H), 7.94 (m, 1H), 7.60 (dd, J = 8.8 Hz, J = 2.5 Hz, 1H), 7.41 (dd, J = 8.6 Hz, J = 1.4 Hz, 1H), 7.34 (d, J = 8.6 Hz, 1H), 7.02 (d, J = 8.8 Hz, 1H), 6.94 (s, 1H), 2.38 (s, 3H). ^{13}C NMR (100 MHz, DMSO-d_6): δ 160.8, 156.2, 147.2, 137.2, 137.1, 136.2, 133.0, 131.5, 130.8, 129.4, 120.6, 119.8, 115.1, 111.3, 104.2, 83.4, 14.3. HRMS calcd for $(C_{17}H_{13}{}^{79}BrIN_3O_2-H)^-$ 495.9163, found 495.9143.

4.1.1.7. 5-Bromo-2-hydroxy-*N*′-{(1*E*)-1-[5-(trifluoromethyl)-1*H*-indol-2-yl]ethylidene}benzohydrazide (6f). Compound **6f** was prepared from 1-[5-(trifluoromethyl)-1*H*-indol-2-yl]ethanone (**3f**) and **5c** using general **Procedure D.**

Yield: 90%, beige solid. Mp = 268–270 °C. ^{1}H NMR (500 MHz, DMSO-d_6): δ 12.14 (s, 1H), 11.79 (s, 1H), 11.42 (s, 1H), 8.09 (d, J = 2.7 Hz, s), 7.97 (d, J = 1.4 Hz, 1H), 7.67 (d, J = 8.7 Hz, 1H), 7.60 (dd, J = 8.7 Hz, J = 2.7 Hz, 1H), 7.44 (dd, J = 8.7 Hz, J = 1.4 Hz, 1H), 7.14 (m, 1H), 7.02 (d, J = 8.7 Hz, 1H), 2.41 (s, 3H). ^{13}C NMR (100 MHz, DMSO-d_6): δ 160.9, 156.3, 147.0, 139.6, 138.4, 136.2, 133.1, 127.4, 125.9 (q, J = 271 Hz, 1C), 120.6 (m, 1C), 119.8 (m, 1C), 118.8 (m, 1C), 113.3, 111.2, 105.8, 14.2. HRMS calcd for $(C_{18}H_{13}{}^{79}BrF_3N_3O-H)^-$ 438.0070, found 438.0089.

4.1.1.8. (*E*)-5-Bromo-2-hydroxy-*N*′-(1-(5-hydroxy-1*H*-indol-2-yl)ethylidene)benzohydrazide (6g). Compound **6g** was prepared from 1-(5-hydroxy-1*H*-indol-2-yl)ethanone (**3j**) and **5c** using general **Procedure C.**

Yield = 65% (filtration), pale yellow solid. Mp = 190–192 °C. ^{1}H NMR (600 MHz, DMSO-d_6): δ 12.10 (br s, 1H), 11.27 (s, 1H), 11.01 (s, 1H), 8.71 (s, 1H), 8.09 (d, J = 2.3 Hz, 1H), 7.59 (dd,

J = 2.5 Hz, 8.7 Hz, 1H), 7.28 (d, *J* = 8.7 Hz, 1H), 7.01 (d, *J* = 8.7 Hz, 1H), 6.85 (d, *J* = 1.6 Hz, 1H), 6.79 (s, 1H), 6.68 (dd, *J* = 1.9 Hz, 8.7 Hz, 1H), 2.34 (s, 3H). ^{13}C NMR (150 MHz, DMSO-d_6): δ 160.2, 155.7, 150.8, 147.6, 135.8, 135.6, 132.5, 132.4, 128.2, 120.3, 119.3, 114.0, 112.6, 110.8, 104.1, 103.9, 13.8. HRMS calcd for $(C_{17}H_{14}{}^{79}BrN_3O_3+H)^+$ 388.0291, found 388.0284.

4.1.1.9. (*E*)-5-Bromo-2-hydroxy-*N*′-(1-(5-methoxy-1*H*-indol-2-yl)ethylidene)benzohydrazide (6h). Compound **6h** was prepared from 1-(5-methoxy-1*H*-indol-2-yl)ethanone (**3s**) and **5c** using general **Procedure A.**

Yield = 79% (filtration), pale yellow cotton. Mp = 250–251 °C. ^{1}H NMR (600 MHz, DMSO-d_6): δ 12.14 (br s, 1H), 11.30 (s, 1H), 11.20 (s, 1H), 8.09 (d, *J* = 2.4 Hz, 1H), 7.59 (dd, *J* = 8.7 Hz, 2.7 Hz, 1H), 7.37 (d, *J* = 9.0 Hz, 1H), 7.03 (d, *J* = 1.8 Hz, 1H), 7.01 (d, *J* = 8.4 Hz, 1H), 6.88 (d, *J* = 0.8 Hz, 1H), 6.80 (dd, *J* = 9.0 Hz, 2.4 Hz, 1H), 3.75 (s, 3H), 2.36 (s, 3H). ^{13}C NMR (100 MHz, DMSO-d_6): δ 160.2, 155.7, 153.5, 147.4, 136.0, 135.6, 133.0, 132.6, 127.9, 120.3, 119.3, 113.9, 112.9, 110.9, 104.6, 101.6, 55.2, 13.8. HRMS calcd for $(C_{18}H_{16}{}^{79}BrN_3O_3+H)^+$ 402.0448, found 402.0450.

4.1.1.10. (*E*)-5-Bromo-2-hydroxy-*N*′-(1-(5-phenyl-1*H*-indol-2-yl)ethylidene)benzohydrazide (6i). Compound **6i** was prepared from 1-(5-phenyl-1*H*-indol-2-yl)ethanone (**3g**) and **5c** using general **Procedure A.**

Yield = 92% (filtration), beige solid. Mp = 275–276 °C. ^{1}H NMR (600 MHz, DMSO-d_6): δ 12.14 (br s, 1H), 11.42 (s, 1H), 11.33 (s, 1H), 8.10 (d, *J* = 2.4 Hz, 1H), 7.83 (s, 1H), 7.67 (d, *J* = 7.2 Hz, 2H), 7.60 (dd, *J* = 8.7 Hz, 2.7 Hz, 1H), 7.57 (d, *J* = 9.0 Hz, 1H), 7.48 (dd, *J* = 8.4 Hz, 1.2 Hz, 1H), 7.45 (t, *J* = 7.5 Hz, 1H), 7.31 (t, *J* = 7.2 Hz, 1H), 7.05 (s, 1H), 7.02 (d, *J* = 9.0 Hz, 1H), 2.40 (s, 3H). ^{13}C NMR (150 MHz, DMSO-d_6): δ 160.3, 155.6, 147.2, 141.6, 137.4, 136.5, 135.7, 132.6, 131.9, 128.8 (2CH), 128.2, 126.7 (2CH), 126.3, 122.7, 120.3, 119.3, 118.6, 112.6, 110.9, 105.2, 13.8. HRMS calcd for $(C_{23}H_{18}{}^{79}BrN_3O_2+Na)^+$ 470.0480, found 470.0455.

4.1.1.11. (*E*)-5-Bromo-*N*′-(1-(6-bromo-1*H*-indol-2-yl)ethylidene)-2-hydroxybenzohydrazide (6j). Compound **6j** was prepared from 1-(6-bromo-1*H*-indol-2-yl)ethanone (**3i**) and **5c** using general **Procedure C.**

Yield = 50% (after reverse-phase HPLC (acetonitrile/H_2O-0.1% TFA, 80–100% for 15 min, 20 mL/min, 254 nm detection for 18 min), pale yellow solid. Mp = 338–340 °C. ^{1}H NMR (600 MHz, DMSO-d_6): δ 12.17 (br s, 1H), 11.58 (br s, 1H), 11.44 (s, 1H), 8.07 (d, *J* = 2.3 Hz, 1H), 7.66 (s, 1H), 7.57 (dd, *J* = 2.4 Hz, 8.6 Hz, 1H), 7.52 (d, *J* = 8.4 Hz, 1H), 7.13 (dd, *J* = 1.8 Hz, 8.4 Hz, 1H), 7.00 (s, 1H), 6.99 (d, *J* = 9.3 Hz, 1H), 2.37 (s, 3H). ^{13}C NMR (150 MHz, DMSO-d_6): δ 160.5, 156.3, 146.5, 138.5, 136.7, 135.6, 132.5, 126.6, 122.4, 122.2, 120.2, 119.5, 115.8, 114.5, 110.3, 104.8, 13.7. HRMS calcd for $(C_{17}H_{13}{}^{79}Br_2N_3O_2+H)^+$ 451.9428, found 451.9410.

4.1.1.12. (*E*)-5-Bromo-*N*′-(1-(5,6-difluoro-1*H*-indol-2-yl)ethylidene)-2-hydroxybenzohydrazide (6k). Compound **6k** was prepared from 1-(5,6-difluoro-1*H*-indol-2-yl)ethanone (**3c**) and **5c** using general **Procedure A.**

Yield = 55% (filtration), pale yellow powder. Mp = 271–272 °C. ^{1}H NMR (400 MHz, DMSO-d_6): δ 12.11 (br s, 1H), 11.48 (s, 1H), 11.34 (br s, 1H), 8.08 (d, *J* = 2.4 Hz, 1H), 7.61–7.54 (m, 2H), 7.39 (dd, *J* = 11.0 Hz, 7.0 Hz, 1H), 7.01 (d, *J* = 8.8 Hz, 1H), 6.98 (d, *J* = 1.6 Hz, 1H), 2.36 (s, 3H). ^{13}C NMR (150 MHz, DMSO-d_6): δ 160.3, 155.7, 147.7 (dd, *J* = 238 Hz, 16 Hz), 146.5, 145.4 (dd, *J* = 234 Hz, 15 Hz), 137.6 (d, *J* = 4 Hz), 135.7, 133.0 (d, *J* = 11 Hz), 132.6, 122.9 (d, *J* = 9 Hz), 120.2, 119.3, 110.8, 107.1 (d, *J* = 19 Hz), 104.8, 99.7 (d, *J* = 22 Hz), 13.6. HRMS calcd for $(C_{17}H_{12}{}^{79}BrF_2N_3O_2+H)^+$ 408.0159, found 408.0129.

4.1.1.13. (*E*)-5-Bromo-*N*′-(1-(4,5-difluoro-1*H*-indol-2-yl)ethylidene)-2-hydroxybenzohydrazide (6l). Compound **6l** was prepared from 1-(4,5-difluoro-1*H*-indol-2-yl)ethanone (**3d**) and **5c** using general **Procedure A.**

Yield = 75% (filtration), beige powder. Mp = 275–276 °C. ^{1}H NMR (400 MHz, DMSO-d_6): δ 12.11 (br s, 1H), 11.71 (s, 1H), 11.35 (s, 1H), 8.08 (d, *J* = 2.8 Hz, 1H), 7.60 (dd, *J* = 8.8 Hz, 2.8 Hz, 1H), 7.29 (dd, *J* = 9.0 Hz, 3.4 Hz, 1H), 7.18 (td, *J* = 11.6 Hz, 8.0 Hz, 1H), 7.12 (d, *J* = 1.6 Hz, 1H), 7.02 (d, *J* = 8.4 Hz, 1H), 2.39 (s, 3H). ^{13}C NMR (150 MHz, DMSO-d_6): δ 160.3, 155.6, 146.4, 143.1 (dd, *J* = 231 Hz, 11 Hz), 141.9 (dd, *J* = 245 Hz, 14 Hz), 137.9, 135.8 (d, *J* = 9 Hz), 135.7, 132.6, 120.2, 119.3, 117.5 (d, *J* = 18 Hz), 112.7 (d, *J* = 21 Hz), 110.8, 108.4 (dd, *J* = 7 Hz, 4 Hz), 100.3 (d, *J* = 5 Hz), 13.6. HRMS calcd for $(C_{17}H_{12}{}^{79}BrF_2N_3O_2+H)^+$ 408.0154, found 408.0161.

4.1.1.14. (*E*)-5-Bromo-*N*′-(1-(7-fluoro-1*H*-indol-2-yl)ethylidene)-2-hydroxybenzohydrazide (6m). Compound **6m** was prepared from 1-(7-fluoro-1*H*-indol-2-yl)ethanone (**3b**) and **5c** using general **Procedure A.**

Yield = 86% (filtration), beige powder. Mp = 263–264 °C. ^{1}H NMR (400 MHz, DMSO-d_6): δ 12.11 (br s, 1H), 11.75 (s, 1H), 11.34 (s, 1H), 8.08 (d, *J* = 1.6 Hz, 1H), 7.60 (dd, *J* = 8.8 Hz, 2.4 Hz, 1H), 7.42–7.38 (m, 1H), 7.08 (br s, 1H), 7.03–6.97 (m, 3H), 2.40 (s, 3H). ^{13}C NMR (100 MHz, DMSO-d_6): δ 160.5, 155.7, 149.0 (d, *J* = 244 Hz), 147.1, 137.4, 135.7 (d, *J* = 4 Hz), 132.5 (d, *J* = 3 Hz), 131.5 (d, *J* = 6 Hz), 125.5 (d, *J* = 13 Hz), 120.2, 119.7, 119.3 (d, *J* = 8 Hz), 116.9 (d, *J* = 8 Hz), 110.8, 108.0 (d, *J* = 16 Hz), 105.3 (d, *J* = 8 Hz), 14.0. HRMS calcd for $(C_{17}H_{13}{}^{79}BrFN_3O_2+H)^+$ 390.0248, found 390.0250.

4.1.1.15. (*E*)-5-Bromo-2-hydroxy-*N*′-(1-(4,5,6-trifluoro-1*H*-indol-2-yl)ethylidene)benzohydrazide (6n). Compound **6n** was prepared from 1-(4,5,6-trifluoro-1*H*-indol-2-yl)ethanone (**3e**) and **5c** using general **Procedure A.**

Yield = 46% (after column 50/50 hexanes/EtOAc then 90/10 DCM/MeOH), beige powder. ^{1}H NMR (400 MHz, DMSO-d_6): δ 12.10 (br s, 1H), 11.78 (br s, 1H), 11.34 (s, 1H), 8.08 (d, *J* = 2.4 Hz, 1H), 7.60 (dd, *J* = 8.8 Hz, 2.4 Hz, 1H), 7.28 (dd, *J* = 10.2 Hz, 6.2 Hz, 1H), 7.15 (d, *J* = 2.0 Hz, 1H), 7.02 (d, *J* = 8.8 Hz, 1H), 2.38 (s, 3H). ^{13}C NMR (150 MHz, DMSO-d_6): δ 160.3, 155.6, 148.0 (dd, *J* = 239 Hz, 13 Hz), 146.0, 142.7 (ddd, *J* = 247 Hz, 11 Hz, 5 Hz), 137.8 (d, *J* = 3 Hz), 135.6, 133.7 (ddd, *J* = 235 Hz, 18 Hz, 14 Hz), 132.7 (t, *J* = 12 Hz), 132.5, 120.2, 119.2, 113.2 (d, *J* = 18 Hz), 110.8, 100.3, 95.5 (dd, *J* = 22 Hz, 3 Hz), 13.5. HRMS calcd for $(C_{17}H_{11}{}^{79}BrF_3N_3O_2+H)^+$ 426.0060, found 426.0070.

4.1.1.16. (*E*)-*N*′-(1-(1*H*-indol-2-yl)ethylidene)-3-bromobenzohydrazide (6o). Compound **6o** was prepared from 1-(1*H*-indol-2-yl)ethanone **3p** and 5-bromobenzohydrazide (**5d**) using general **Procedure C**.

Yield = 70% (after flash chromatography 3/1; hexanes/EtOAc), pale yellow solid. Mp = 219–224 °C. ^{1}H NMR (600 MHz, DMSO-d_6): δ 11.31 (s, 1H), 10.89 (s, 1H), 8.09 (br s, 1H), 7.92 (d, *J* = 7.6 Hz, 1H), 7.81 (d, *J* = 8.0 Hz,1H), 7.57 (d, *J* = 7.9 Hz, 1H), 7.51 (t, *J* = 7.9 Hz, 1H), 7.49 (d, *J* = 7.3 Hz, 1H), 7.16 (dt, *J* = 0.7 Hz, 7.2 Hz, 1H), 7.01 (dt, *J* = 0.9 Hz, 7.5 Hz, 1H), 6.99 (br s, 1H), 2.43 (s, 3H). ^{13}C NMR (150 MHz, DMSO-d_6): δ 163.1, 151.9, 138.5, 137.2, 136.8, 135.1, 131.5, 131.3, 128.5, 128.0, 124.1, 122.5, 121.6, 120.3, 113.1, 105.8, 15.4. HRMS calcd for $(C_{17}H_{14}{}^{79}BrN_3O+H)^+$ 356.0393, found 356.0394.

4.1.1.17. (*E*)-*N*′-(1-(1*H*-Indol-2-yl)ethylidene)-2-hydroxybenzohydrazide (6p). Compound **6p** was prepared from 1-(1*H*-indol-2-yl)ethanone (**3p**) and 2-hydroxybenzohydrazide (**5e**) using general **Procedure C**.

Yield = 54% (after flash chromatography 40/1; DCM/MeOH), pale yellow solid. Mp = 246–248 °C. ^{1}H NMR (600 MHz, DMSO-d_6): δ 11.86 (br s, 1H), 11.38 (br s, 1H), 11.31 (s, 1H), 8.03 (dd, J = 1.4 Hz, 7.8 Hz, 1H), 7.56 (d, J = 7.9 Hz, 1H), 7.50 (d, J = 8.1 Hz, 1H), 7.43 (dt, J = 1.8 Hz, 7.2 Hz, 1H), 7.14 (dt, J = 1.1 Hz, 8.1 Hz, 1H), 7.04 (d, J = 7.6 Hz, 1H), 7.002 (t, J = 7.9 Hz, 1H), 7.001 (t, J = 7.0 Hz, 1H), 6.97 (d, J = 1.5 Hz, 1H), 2.39 (s, 3H). ^{13}C NMR (150 MHz, DMSO-d_6): δ 162.3, 157.1, 147.2, 138.2, 136.4, 133.8, 131.0, 128.1, 123.6, 121.1, 120.1, 119.8, 118.4, 117.4, 112.6, 105.1, 14.3. HRMS calcd for $(C_{17}H_{15}N_3O_2+H)^+$ 294.1237, found 294.1237.

4.1.1.18. (*E*)-*N*′-(1-(1*H*-Indol-2-yl)ethylidene)-4-bromo-2-hydroxybenzohydrazide (6q). Compound **6q** was prepared from **3p** and 4-bromo-2-hydroxy-benzohydrazide (**5l**) using general **Procedure C**.

Yield = 62% (filtration), yellow solid. Mp = 281–284 °C. ^{1}H NMR (600 MHz, DMSO-d_6): δ 12.27 (br s, 1H), 11.31 (s, 1H), 11.25 (s, 1H), 7.94 (d, J = 8.4 Hz, 1H), 7.55 (d, J = 7.9 Hz, 1H), 7.49 (d, J = 8.2 Hz, 1H), 7.22 (d, J = 1.7 Hz, 1H), 7.20 (dd, J = 1.7 Hz, 8.4 Hz, 1H), 7.14 (dt J = 0.9 Hz, 7.6 Hz, 1H), 7.00 (dt, J = 0.9 Hz, 7.5 Hz, 8.7 Hz, 1H), 6.98 (d, J = 1.2 Hz, 1H), 2.38 (s, 3H). ^{13}C NMR (150 MHz, DMSO-d_6): δ 161.8, 158.1, 148.0, 138.7, 136.7, 133.4, 128.5, 126.8, 124.1, 123.6, 121.6, 120.3, 120.2, 118.7, 113.1, 105.7, 14.7. HRMS calcd for $(C_{17}H_{14}{}^{79}BrN_3O_2+H)^+$ 372.0342, found 372.0347.

4.1.1.19. (*E*)-*N*′-(1-(1*H*-Indol-2-yl)ethylidene)benzohydrazide (6r). Compound **6r** was prepared from **3p** and benzohydrazide (**5f**) using general **Procedure C**.

Yield = 62%, pale yellow solid. Mp = 224–226 °C. ^{1}H NMR (600 Mz, DMSO): δ 11.29 (br s, 1H), 10.8 (s, 1H), 7.92 (d, J = 7.3 Hz, 2H), 7.60 (t, J = 7.3 Hz, 1H), 7.58 – 7.52 (m, 3H), 7.48 (d, J = 8.1 Hz, 1H), 7.14 (dt, J = 0.9 Hz, 7.6 Hz, 1H), 7.00 (dt, J = 0.8 Hz, 7.4 Hz, 1H), 6.96 (br s, 1H), 2.42 (s, 3H). ^{13}C NMR (150 Mz, DMSO): δ 164.1, 150.8, 138.1, 136.5, 134.6, 132.0, 128.8, 128.3, 128.0, 123.6, 121.2, 119.8, 112.6, 105.1, 14.9. HRMS calcd for $(C_{17}H_{15}N_3O+H)^+$ 278.1288, found 278.1278.

4.1.1.20. (*E*)-*N*′-(1-(1*H*-Indol-2-yl)ethylidene)picolinohydrazide (6s). Compound **6s** was prepared from **3p** and picolinohydrazide (**5g**) using general **Procedure C**.

Yield = 87%, yellow solid. Mp = 219–221 °C. ^{1}H NMR (600 MHz, DMSO): δ 11.36 (s, 1H), 11.12 (s, 1H), 8.74 (d, J = 4.7 Hz, 1H), 8.18 (d, J = 7.8 Hz,1H), 8.08 (dt, J = 1.7 Hz, 7.7 Hz, 1H), 7.70 (ddd, J = 1.2 Hz, 4.7 Hz, 5.9 Hz, 1H), 7.57 (d, J = 7.9 Hz, 1H), 7.50 (dd, J = 0.8 Hz, 8.2 Hz, 1H), 7.15 (dt, J = 1.1 Hz, 7.0 Hz, 1H), 7.01 – 6.99 (m, 2H), 2.45 (s, 3H). ^{13}C NMR (150 MHz, DMSO): δ 160.2, 150.3, 149.9, 149.6, 139.2, 138.7, 136.6, 128.5, 128.1, 124.2, 123.2, 121.7, 120.3, 113.1, 106.0, 14.3. HRMS calcd for $(C_{16}H_{14}N_4O+H)^+$ 279.1240, found 279.1243.

4.1.1.21. (*E*)-*N*′-(1-(1*H*-Indol-2-yl)ethylidene)-2-hydroxy-5-iodobenzohydrazide (6u). Compound **6u** was prepared from **3p** and 2-hydroxy-5-iodobenzohydrazide (**5h**) using general **Procedure C**.

Yield = 32% (after flash chromatography 4/1 → 1/1; hexanes/EtOAc), pale yellow solid. Mp = 251–255 °C. ^{1}H NMR (600 MHz, DMSO-d_6): δ 12.10 (br s, 1H), 11.32 (s, 2H), 8.25 (d, J = 2.2 Hz, 1H), 7.72 (dd, J = 2.3 Hz, 8.5 Hz, 1H), 7.56 (d, J = 7.9 Hz, 1H), 7.49 (d, J = 8.0 Hz, 1H), 7.14 (dt, J = 1.0 Hz, 7.1 Hz, 1H), 7.00 (dt, J = 0.9 Hz, 7.4 Hz, 1H), 6.98 (s, 1H), 6.89 (d, J = 8.6 Hz, 1H), 2.38 (s, 3H). ^{13}C NMR (150 MHz, DMSO-d_6): δ 161.2, 157.3, 148.1, 142.2, 139.4, 138.7, 136.7, 128.5, 124.1, 121.6, 120.6, 120.3, 113.1, 105.7, 82.6, 14.7. HRMS calcd for $(C_{17}H_{14}IN_3O_2+H)^+$ 420.0203, found 420.0201.

4.1.1.22. 4-Hydroxy-*N*′-[(1*E*)-1-(1*H*-Indol-2-yl)ethylidene]-1,1′-biphenyl-3-carbohydrazide (6v). Compound **6v** was prepared from **3p**, hydrazine hydrate and methyl 4-hydroxy-1,1′-biphenyl-3-carboxylate using general **Procedure E**.

Yield: 22%, off-white solid. Mp = 274–276 °C. ^{1}H NMR (400 MHz, DMSO-d_6): δ 12.02 (br s, 1H), 11.48 (s, 1H), 11.36 (s, 1H), 8.28 (d, J = 2.3 Hz, 1H), 7.76 (dd, J = 8.6 Hz, J = 2.3 Hz, 1H), 7.66 (d, J = 7.3 Hz, 2H), 7.57 (d, J = 7.6 Hz, 1H), 7.50 (d, J = 7.6 Hz, 1H), 7.48 (d, J = 7.3 Hz, 2H), 7.35 (t, J = 7.3 Hz, 1H), 7.16 (t, J = 7.6 Hz, 1H), 7.14 (d, J = 8.6 Hz, 1H), 7.00 (t, J = 7.6 Hz, 1H), 6.90 (br s, 1H), 2.42 (s, 3H). ^{13}C NMR (100 MHz, DMSO-d_6): δ 162.3, 156.8, 147.9, 139.8, 138.2, 136.3, 132.2, 132.0, 129.4, 128.8, 128.1, 127.5, 126.7, 123.6, 121.1, 119.8, 118.7, 118.1, 112.6, 105.2, 14.4. HRMS calcd for $(C_{23}H_{19}N_3O_2+H)^+$ 370.1550, found 370.1416.

4.1.1.23. (*E*)-*N*′-(1-(1*H*-Indol-2-yl)ethylidene)-5-bromo-2-methoxybenzohydrazide (6w). Compound **6w** was prepared from **3p** and 2-methoxy-4-bromobenzohydrazide (**5i**) using general **Procedure C**.

Yield = 41% (filtration), pale yellow solid. Mp = 241–244 °C. ^{1}H NMR (600 MHz, DMSO-d_6): δ 11.31 (s, 1H), 10.90 (s, 1H), 7.96 (d, J = 2.6 Hz, 1H), 7.73 (dd, J = 2.7 Hz, 8.8 Hz, 1H), 7.56 (d, J = 8.1 Hz, 1H), 7.49 (d, J = 8.1 Hz, 1H), 7.23 (d, J = 8.9 Hz, 1H), 7.14 (dt, J = 1.0 Hz, 7.6 Hz, 1H), 7.00 (dt, J = 0.8 Hz, 7.5 Hz, 1H), 7.23 (d, J = 8.9 Hz, 1H), 6.98 (d, J = 1.5 Hz, 1H), 3.99 (s, 3H), 2.38 (s, 3H). ^{13}C NMR (150 MHz, DMSO-d_6): δ 160.3, 156.84, 148.0, 138.2, 136.3, 135.5, 133.1, 128.1, 124.7, 123.6, 121.1, 119.8, 115.4, 112.8, 112.6, 105.3, 57.3, 14.2. HRMS calcd for $(C_{18}H_{16}{}^{79}BrN_3O_2+H)^+$ 386.0499, found 386.0515.

4.1.1.24. (*E*)-*N*′-[1-(1*H*-indol-2-yl)ethylidene]-5-bromo-2-ethoxybenzohydrazide (6x). Compound **6x** was prepared from 1-(*1H*-indol-2-yl)ethanone **3p**, hydrazide hydrate and methyl 5-bromo-2-ethoxybenzoate using general **Procedure E**.

Yield: 84%, beige solid. Mp = 260–262 °C. ^{1}H NMR (400 MHz, DMSO-d_6): δ 11.32 (br s, 1H), 10.81 (s, 1H), 8.01 (d, J = 2.3 Hz, 1H), 7.71 (dd, J = 8.9 Hz, J = 2.3 Hz, 1H), 7.56 (d, J = 7.6 Hz, 1H), 7.49 (d, J = 7.6 Hz, 1H), 7.22 (d, J = 8.9 Hz, 1H), 7.14 (d, J = 7.6 Hz, 1H), 6.99 (t, J = 7.6 Hz, 1H), 6.98 (s, 1H), 4.26 (q, J = 7.0 Hz, 2H), 2.39 (s, 3H), 1.47 (t, J = 7.0 Hz, 3H). ^{13}C NMR (100 MHz, DMSO-d_6): δ 159.8, 155.7, 147.1, 137.7, 135.8, 135.2, 133.0, 127.5, 123.8, 123.1, 120.6, 119.3, 115.5, 112.2, 112.1, 104.8, 65.2, 14.6, 13.9. HRMS calcd for $(C_{19}H_{18}{}^{79}BrN_3O+Na)^+$ 422.0475, found 422.0464.

4.1.1.25. (*E*)-*N*′-(1-(1*H*-indol-2-yl)ethylidene)-5-bromo-2-(prop-2-ynyloxy)benzohydrazide (6z). Compound **6z** was prepared from **3p** and **5a** using general **Procedure A**.

Yield = 54% (filtration), off-white solid. Mp = 246–251 °C. ^{1}H NMR (600 MHz, DMSO-d_6): δ 11.30 (s, 1H), 10.78 (s, 1H), 7.93 (d, J = 2.6 Hz, 1H), 7.75 (dd, J = 2.6 Hz, 8.9 Hz, 1H), 7.56 (d, J = 7.9 Hz, 1H), 7.49 (d, J = 8.1 Hz, 1H), 7.26 (d, J = 8.9 Hz, 1H), 7.14 (dt, J = 0.9 Hz, 8.0 Hz, 1H), 7.00 (dt, J = 0.7 Hz, 7.8 Hz, 1H), 6.97 (d, J = 1.5 Hz, 1H), 5.04 (d, J = 2.3 Hz, 1H), 3.75 (t, J = 2.3 Hz, 1H), 2.39 (s, 3H). ^{13}C NMR (150 MHz, DMSO-d_6): δ 160.8, 155.2, 148.7, 138.7, 136.7, 135.7, 133.6, 128.5, 126.2, 124.1, 121.6, 120.2, 117.0, 114.0, 113.1, 105.7, 80.5, 79.3, 58.2, 15.0. HRMS calcd for $(C_{20}H_{16}{}^{81}BrN_3O_2+H)^+$ 412.0481, found 412.0467.

4.1.1.26. (*E*)-*N*′-(1-(1*H*-indol-2-yl)ethylidene)-3,5-dibromo-2-hydroxybenzohydrazide (6α). Compound **6α** was prepared from **3p** and 3,5-dibromo-2-hydroxybenzohydrazide (**5j**) using general **Procedure A**.

Yield = 55% (filtration), pale yellow solid. Mp = 146–150 °C. ^{1}H NMR (600 MHz, DMSO-d_6): δ 11.64 (br s, 1H), 11.39 (s, 1H), 8.16 (d, J = 1.6 Hz, 1H), 7.99 (d, J = 1.8 Hz, 1H), 7.58 (d, J = 7.9 Hz, 1H),

7.48 (d, J = 8.2 Hz, 1H), 7.17 (t, J = 7.9 Hz, 1H), 7.05 (s, 1H), 7.00 (t, J = 7.8 Hz, 1H), 2.44 (s, 3H). ^{13}C NMR (150 MHz, DMSO-d_6): δ 163.8, 156.6, 153.5, 138.6, 138.2, 135.8, 130.7, 128.0, 124.0, 121.4, 119.9, 119.2, 113.3, 112.7, 110.1, 106.2, 15.2. HRMS calcd for $(C_{17}H_{13}{}^{79}Br_2N_3O_2+H)^+$ 451.9428, found 451.9431.

4.1.1.27. (*E*)-*N*′-[1-(1*H*-Indol-2-yl)ethylidene]-2-hydroxy-3,5-diisopropylbenzohydrazide (6χ). Compound **6χ** was prepared from **3p**, hydrazine hydrate and ethyl 2-hydroxy-3,5-diisopropylbenzoate using general **Procedure E**.

Yield: 80%, yellow solid. Mp = 106–108 °C. ^{1}H NMR (400 MHz, DMSO-d_6): δ 12.35 (s, 1H), 11.40 (s, 1H), 11.12 (s, 1H), 7.67 (d, J = 2.3 Hz, 1H), 7.59 (d, J = 7.6 Hz, 1H), 7.49 (d, J = 7.6 Hz, 1H), 7.29 (1H, J = 2.3 Hz, 1H), 7.17 (t, J = 7.6 Hz, 1H), 7.04 (br s, 1H), 7.02 (t, J = 7.6 Hz, 1H), 3.30 (sept., J = 7.0 Hz, 1H), 2.89 (spet., J = 7.0 Hz, 1H), 1.24 (d, J = 7.0 Hz, 6H), 1.22 (d, J = 7.0 Hz, 6H). ^{13}C NMR (100 MHz, DMSO-d_6): δ 166.9, 156.4, 144.2, 138.8, 138.1, 136.6, 136.0, 129.1, 128.0, 123.9, 123.0, 121.3, 119.9, 114.1, 112.6, 105.8, 33.5, 26.7, 22.9, 19.0, 15.2. HRMS calcd for $(C_{19}H_{18}{}^{79}BrN_3O_2+Na)^+$ 400.1995, found 400.1999.

4.1.1.28. (*E*)-*N*′-(1-(1*H*-indol-2-yl)ethylidene)-5-bromo-2-hydroxy-4-methoxybenzohydrazide (6δ). Compound **6δ** was prepared from **3p** and 5-bromo-2-hydroxy-4-methoxybenzohydrazide (**5k**) using general **Procedure C**.

Yield = 82% (filtration), pale yellow solid. Mp = 242–244 °C. ^{1}H NMR (600 MHz, DMSO-d_6): δ 12.40 (br s, 1H), 11.31 (s, 1H), 11.17 (br s, 1H), 8.17 (s, 1H), 7.56 (d, J = 7.9 Hz, 1H), 7.48 (d, J = 8.2 Hz, 1H), 7.16 (dt, J = 0.9 Hz, 7.6 Hz, 1H), 6.99 (t, J = 7.1 Hz, 1H), 6.97 (s, 1H), 6.69 (s, 1H), 3.88 (s, 3H), 2.38 (s, 3H). ^{13}C NMR (150 MHz, DMSO-d_6): δ 161.1, 158.8, 158.4, 147.4, 137.7, 135.8, 133.7, 127.6, 123.1, 120.6, 119.3, 112.1, 111.4, 104.7, 100.9, 100.6, 56.5, 13.8. HRMS calcd for $(C_{18}H_{16}{}^{79}BrN_3O_3+H)^+$ 402.0448, found 402.0454.

4.1.1.29. (*E*)-*N*′-((1*H*-Indol-2-yl)methylene)-5-bromo-2-hydroxybenzohydrazide (6ε). Compound **6ε** was prepared from 1*H*-indole-2-carbaldehyde **3o** (obtained by reduction and oxidation of 1*H*-indole-2-carboxylic acid, cf. scheme) and 5-bromo-2-hydroxybenzohydrazide (**5c**) using general **Procedure A**.

Yield = 78% (filtration), pale yellow powder. Mp = 257–258 °C. ^{1}H NMR (400 MHz, DMSO-d_6): δ 11.95 (br s, 1H), 11.84 (s, 1H), 11.62 (s, 1H), 8.48 (s, 1H), 8.05 (d, J = 2.8 Hz, 1H), 7.59 (dd, J = 8.8 Hz, 2.4 Hz, 1H), 7.57 (d, J = 8.0 Hz, 1H), 7.17 (t, J = 7.4 Hz, 1H), 7.02 (t, J = 7.4 Hz, 1H), 6.97 (d, J = 8.8 Hz, 1H), 6.89 (d, J = 1.2 Hz, 1H). ^{13}C NMR (100 MHz, DMSO-d_6): δ 163.0, 157.9, 141.8, 138.0, 136.0, 132.8, 130.8, 127.6, 123.5, 120.8, 119.6 (2CH), 112.1, 110.0, 107.6. HRMS calcd for $(C_{16}H_{12}{}^{79}BrN_3O_2+H)^+$ 358.0186, found 358.0200.

4.1.1.30. (*E*)-*N*′-(1-(1*H*-indol-2-yl)propylidene)-5-bromo-2-hydroxybenzohydrazide (6ϕ). Compound **6ϕ** was prepared from 1-(1*H*-indol-2-yl)propan-1-one **3t** (obtained by addition of ethylmagnesium bromide to the Weinreb amide **2**, cf. scheme) and 5-bromo-2-hydroxybenzohydrazide (**5c**) using general **Procedure A**.

Yield = 73% (filtration), white powder. Mp = 255–256 °C. ^{1}H NMR (400 MHz, DMSO-d_6): δ 12.16 (br s, 1H), 11.48 (br d, J = 0.8 Hz, 1H), 11.28 (s, 1H), 8.09 (d, J = 2.4 Hz, 1H), 7.59 (dd, J = 8.6 Hz, 2.6 Hz, 1H), 7.56 (d, J = 8.0 Hz, 1H), 7.49 (d, J = 8.0 Hz, 1H), 7.14 (td, J = 7.8 Hz, 0.6 Hz, 1H), 7.04–6.97 (m, 3H), 2.82 (q, J = 7.6 Hz, 2H), 1.24 (t, J = 7.6 Hz, 3H). ^{13}C NMR (100 MHz, DMSO-d_6): δ 160.0, 155.4, 151.3, 137.8, 135.6, 134.8, 132.7, 127.6, 123.1, 120.6, 120.5, 119.3 (2CH), 112.1, 110.9, 104.4, 20.6, 10.8. HRMS calcd for $(C_{18}H_{16}{}^{79}BrN_3O_2+H)^+$ 386.0499, found 386.0505.

4.1.1.31. (*Z*)-*N*′-(1-(1*H*-Indol-2-yl)-2,2-dimethylpropylidene)-5-bromo-2-hydroxybenzohydrazide (6ι). Compound **6ι** was prepared from 1-(1*H*-indol-2-yl)-2,2-dimethylpropan-1-one (**3u**) (obtained by addition of *t*-BuLi to the Weinreb amide **2**, cf. scheme) and 5-bromo-2-hydroxybenzohydrazide (**5c**) using general **Procedure A**.

Yield = 58% (after column 90/10 hexanes/EtOAc), white powder. Mp = 217–218 °C. ^{1}H NMR (600 MHz, DMSO-d_6): δ 11.35 (s, 1H), 11.01 (s, 2H), 7.98 (d, J = 1.8 Hz, 1H), 7.63 (d, J = 8.4 Hz, 1H), 7.45–7.41 (m, 2H), 7.16 (t, J = 7.8 Hz, 1H), 7.06 (t, J = 7.5 Hz, 1H), 6.77 (d, J = 8.4 Hz, 1H), 6.52 (s, 1H), 1.21 (s, 9H). ^{13}C NMR (150 MHz, DMSO-d_6): δ 159.8, 158.0, 155.0, 136.6, 135.6, 133.0, 127.7, 127.4, 122.1, 120.7, 120.0, 119.5, 119.1, 111.7, 110.8, 102.4, 38.5, 28.1. HRMS calcd for $(C_{20}H_{20}{}^{79}BrN_3O_2\ Na)^+$ 436.0637, found 436.0631.

4.1.1.32. (*E*/*Z*)-*N*′-((1*H*-indol-2-yl)(phenyl)methylene)-5-bromo-2-hydroxybenzohydrazide (6φ). Compound **6φ** was prepared from (1*H*-indol-2-yl)(phenyl)methanone (**3v**) (obtained by addition of PhLi to the Weinreb amide **2**, cf. scheme) and 5-bromo-2-hydroxybenzohydrazide(**5c**) using general **Procedure A**. Yield = 43% (after column 70/30 hexanes/EtOAc), pale yellow powder. NMR analysis indicated that **6μ** is present in two isomeric forms (89:11).

4.1.1.32.1. Major isomer (E). ^{1}H NMR (600 MHz, DMSO-d_6): δ 11.60 (s, 1H), 11.35 (s, 1H), 11.27 (s, 1H), 8.07 (s, 1H), 7.72–7.46 (m, 8H), 7.16 (t, J = 7.2 Hz, 1H), 6.97 (t, J = 6.9 Hz, 1H), 6.85 (d, J = 8.4 Hz, 1H), 6.12 (s, 1H). ^{13}C NMR (150 MHz, DMSO-d_6): δ 159.6, 155.0, 148.4, 137.9, 135.7, 135.5, 133.0, 132.0, 130.1, 129.4 (2CH), 128.3 (2CH), 127.5, 123.5, 120.8, 119.9, 119.5, 119.1, 112.2, 111.0, 107.4.

4.1.1.32.2. Minor isomer (Z). ^{13}C NMR (150 MHz, DMSO-d_6): δ 160.4, 155.7, 146.8, 137.1, 136.9, 135.8, 133.1, 129.9, 128.5 (2CH), 127.9 (2CH), 127.3, 127.2, 123.0, 121.2, 120.0, 119.9, 119.2, 112.1, 110.9, 105.2.

HRMS (mixture) calcd for $(C_{22}H_{16}{}^{79}BrN_3O_2+Na)^+$ 456.0324, found 456.0309.

4.1.1.33. (*E*)-5-Bromo-*N*′-(1-(5-bromo-1*H*-indol-2-yl)propylidene)-2-hydroxybenzohydrazide (6γ). Compound **6γ** was prepared from 1-(5-bromo-1*H*-indol-2-yl)propan-1-one **(3l)** and 5-bromo-2-hydroxybenzohydrazide (**5c**) using general **Procedure C**.

Yield = 41% (after flash chromatography 20/1; DCM/MeOH), pale yellow solid. Mp = 252–254 °C. ^{1}H NMR (600 MHz, DMSO-d_6): δ 12.17 (br s, 1H), 11.60 (br s, 1H), 11.48 (s, 1H), 8.08 (d, J = 2.5 Hz, 1H), 7.75 (d, J = 1.4 Hz, 1H), 7.58 (dd, J = 2.6 Hz, 8.7 Hz, 1H), 7.46 (d, J = 8.6 Hz, 1H), 7.26 (dd, J = 1.9 Hz, 8.6 Hz, 1H), 7.02 (d, J = 8.7 Hz, 1H), 6.95 (s, 1H), 2.81 (q, J = 7.7 Hz, 2H), 1.22 (t, J = 7.6 Hz, 3H). ^{13}C NMR (150 MHz, DMSO-d_6): δ 160.1, 155.7, 150.7, 136.4, 136.2, 135.6, 132.7, 129.5, 125.5, 122.7, 120.5, 119.4, 114.1, 111.7, 110.7, 103.6, 20.6, 10.7. HRMS calcd for $(C_{18}H_{15}{}^{79}Br_2N_3O_2+H)^+$ 465.9584, found 465.9588.

4.1.1.34. Specific procedures for the synthesis of the hydrazides 6. 5-Chloro-2-hydroxy-*N*′-((1*E*)-1-(1*H*-indol-2-yl)ethylidene)benzohydrazide (**6t**)

To a mixture of methyl 5-chloro-2-hydroxybenzoate (162 mg, 0.87 mmol) in isobutanol (0.5 mL) was added hydrazine hydrate (42 μL, 0.87 mmol). The reaction mixture was irradiated with microwaves for 15 min at 115 °C. Isobutanol was added and the supernatant was removed. The residue was taken up in isobutanol (0.5 mL) and 1-(*1H*-indol-2-yl)ethanone **3p** (138 mg, 0.87 mmol) was added. The reaction mixture was again irradiated with microwaves for 10 min at 110 °C. The solid product was filtered and then, triturated with EtOH and Et_2O to afford **6t** as a yellow solid

(90 mg, 33%). Mp = 198–200 °C. ^{1}H NMR (400 MHz, DMSO-d_6): δ 12.46 (s, 1H), 11.39 (s, 1H), 10.07 (s, 1H), 7.86 (d, J = 2.4 Hz, 1H), 7.60 (d, J = 7.6 Hz, 1H), 7.47 (d, J = 7.6 Hz, 1H), 7.41 (dd, J = 8.8 Hz, 2.4 Hz, 1H), 7.19 (tm, J = 7.6 Hz), 7.03 (m, 2H), 6.93 (d, J = 8.8 Hz, 1H), 2.48 (s, 3H). ^{13}C NMR (100 MHz, DMSO-d_6): δ 158.0, 153.8, 137.5, 136.5, 132.8, 127.7, 126.8, 123.4, 122.3, 120.9, 119.3, 119.1, 111.8, 104.9, 14.5. HRMS calcd for $(C_{17}H_{14}{}^{35}ClN_3O_2+Na)^+$ 350.0663, found 350.0667.

4.1.1.35. 5-Bromo-2-(ethoxymethoxy)-*N*′-((1*E*)-1-(1*H*-indol-2-yl)ethylidene)benzohydrazide (6y). To a solution of **6a** (73 mg, 0.20 mmol) in anhydrous THF (30 mL) maintained at 0 °C were added, under an argon atmosphere, NaH (8.1 mg, 60%, 0.24 mmol) and then, after 10 min stirring still at 0 °C, chloromethylethyl ether (45 μL, 0.49 mmol). The mixture was stirred at room temperature for 4 h and then, quenched with a saturated aqueous ammonium chloride solution. The aqueous layer was extracted with EtOAc and the organic layer was dried over anhydrous Na_2SO_4, filtered through a silica gel pad and evaporated under reduced pressure. The residue was triturated with Et_2O to afford **6y** as a pale yellow solid (65 mg, 77%). Mp = 128–130 °C. ^{1}H NMR (400 MHz, DMSO-d_6): δ 11.32 (s, 1H), 10.90 (s, 1H), 7.94 (d, J = 2.5 Hz, 1H), 7.71 (dd, J = 9.0 Hz, 2.5 Hz, 1H), 7.57 (d, J = 7.6 Hz, 1H), 7.50 (d, J = 7.6 Hz, 1H), 7.29 (d, J = 9.0 Hz, 1H), 7.15 (t, J = 7.6 Hz, 1H), 7.00 (t, J = 7.6 Hz, 1H), 6.98 (s, 1H), 5.46 (s, 2H), 3.75 (q, J = 7.0 Hz, 2H), 2.39 (s, 3H), 1.16 (t, J = 7.0 Hz, 3H). ^{13}C NMR (100 MHz, DMSO-d_6): δ 160.0, 153.9, 147.6, 137.7, 135.8, 134.7, 132.5, 127.6, 125.6, 123.1, 120.6, 119.3, 117.6, 113.2, 112.1, 104.8, 93.9, 4.5, 14.9, 13.8. HRMS calcd for $(C_{20}H_{20}{}^{79}BrN_3O_3+Na)^+$ 453.0562, found 453.0561.

4.1.1.36. (*E*)-*N*′-(1-(1*H*-Indol-2-yl)ethylidene)-3,5-dibromo-2-methoxybenzohydrazide (6β). A mixture of 1-(1*H*-indol-2-yl)ethanone **3p** (50 mg, 0.31 mmol) and 3,5-dibromo-2-methoxybenzohydrazide (101 mg, 0.31 mmol) in EtOH (2.5 mL) was irradiated with microwaves at 180 °C for 3 h. The precipitate was filtered and was washed with hot EtOH (2 × 2 mL) to give pale yellow solid (75 mg, 51%). NMR analysis indicated that **6β** is present in two isomeric forms (15:1). ^{1}H NMR (600 MHz, DMSO-d_6): δ 11.30 (br s, 1H), 10.97 (s, 1H), 8.06 (d, J = 2.4 Hz, 1H), 7.79 (d, J = 7.4 Hz, 1H), 7.56 (d, J = 7.9 Hz, 1H), 7.49 (d, J = 8.2 Hz, 1H), 7.14 (t, J = 7.9 Hz, 1H), 7.00 (t, J = 7.7 Hz, 1H), 6.97 (d, J = 1.9 Hz, 1H), 3.86 (s, 3H), 2.36 (s, 3H). ^{13}C NMR (150 MHz, DMSO-d_6): δ 160.9, 154.1, 149.5, 138.2, 137.2, 136.2, 133.3, 132.1, 128.0, 123.7, 121.2, 119.8, 118.8, 117.0, 112.7, 105.4, 62.6, 14.7. HRMS calcd for $(C_{18}H_{15}{}^{79}Br_2N_3O_2+H)^+$ 465.9584, found 465.9597.

4.1.1.37. (*E*)-*N*′-[(1*H*-Indol-2-yl)methylene]-5-bromo-2-methoxybenzohydrazide (6η). To a mixture of methyl 5-bromo-2-methoxybenzoate (1.35 g, 5.50 mmol, 1.0 equiv) in ethanol (0.6 ml) was added hydrazine hydrate (535 μL, 11.00 mmol, 2.0 equiv). The reaction mixture was irradiated with microwaves for 40 min at 100 °C. Ethanol was added and the supernatant was removed. The residue was taken up in ethanol (5 mL) and 1*H*-indole-2-carbaldehyde (0.80 g, 5.50 mmol) was added. The reaction mixture was again irradiated with microwaves for 50 min at 100 °C. The solid product was filtered and then, triturated with ethanol and diethyl ether to afford **6γ** (1.49 g). Yield: 73%, pale yellow solid. Mp = 108–110 °C. ^{1}H NMR (400 MHz, DMSO-d_6): δ 11.59 (s, 1H), 11.55 (s, 1H), 8.36 (s, 1H), 7.74 (d, J = 2.3 Hz, 1H), 7.68 (dd, J = 8.9 Hz, J = 2.3 Hz, 1H), 7.56 (d, J = 7.6 Hz, 1H), 7.44 (d, J = 7.6 Hz, 1H), 7.16 (m, 1H), 7.16 (d, J = 8.9 Hz, 1H), 7.01 (t, J = 7.6 Hz, 1H), 6.83 (br s, 1H), 3.89 (s, 3H). ^{13}C NMR (100 MHz, DMSO-d_6): δ 160.6, 156.0, 140.5, 137.9, 134.4, 133.0, 131.9, 127.6, 125.7, 123.3, 120.7, 119.5, 114.4, 112.0, 111.8, 107.0, 56.2. HRMS calcd for $(C_{17}H_{14}{}^{79}BrN_3O_2+Na)^+$ 394.0162, found 394.0171.

4.2. PK enzymatic assays, cell-based assays and cytotoxicity

Measurements of pyruvate kinase activity, in vitro susceptibility testing and the determination of mammalian cytotoxicity were performed using previously described procedures and statistical analysis.[3]

4.3. X-ray crystallography

Suitable crystals of compounds **6φ** and **6ι** were mounted on the end of a glass fiber with epoxy. Single crystal X-ray crystallographic analysis was performed on a Bruker SMART diffractometer equipped with an APEX II CCD area detector fixed at a distance of 6.0 cm from the crystal and a Mo Kα fine focus sealed tube (λ = 0.71073 nm) operated at 1.5 kW (50 kV, 30 mA) and filtered with a graphite monochromator.

The structures were solved using direct methods (SIR92)[6] and refined by least-squares procedures using CRYSTALS.[7] All hydrogen atoms were placed in idealized geometric positions and linked to their respective carbon atoms using a riding model during refinement. The isotropic temperature factor of each hydrogen atom was initially set to 1.2 times that of the atom it is bonded to and then the temperature factors of groups of similar hydrogen atoms were linked during refinement. Crystal structure diagrams were generated using ORTEP-3 for Windows (v. 2.02).[8]

All crystals diffracted poorly and there was not enough data to model all atoms anisotropically, but the identity and connectivity of the atoms are clear. In **6φ**, the methyl carbon of the ethyl substituent was disordered and modeled accordingly (see CIF file for details). Only the carbon with higher occupancy is shown in Figure 3.

Acknowledgments

The authors acknowledge Genome British Columbia, Genome Canada, the Natural Sciences and Engineering Council of Canada (NSERC) and the Pfizer-CDRD Innovation Fund for financial support.

The authors also acknowledge support of the Vancouver General Hospital and the University of British Columbia Hospital Foundation and SARS Accelerated Vaccine Initiative through the PRoteomics for Emerging PAthogen REsponse (PREPARE) Project. RNY acknowledges the support of Simon Fraser University, the British Columbia Government Leading Edge Endowment Fund and Merck Frosst Canada Ltd.

Supplementary data

PDP ID Codes: Crystallographic data for compound **8d**: ID 3T0T.

CCDC 873762–873763 contains the supplementary crystallographic data compounds **6φ** and **6ι**. These data can be obtained free of charge from The Cambridge Crystallographic Data Centre via www.ccdc.cam.ac.uk/data_request/cif.

Supplementary data associated with this article can be found, in the online version, at http://dx.doi.org/10.1016/j.bmc.2012.10.002.

References and notes

1. Cherkasov, A.; Hsing, M.; Zoraghi, R.; Foster, L. J.; See, R. H.; Stoynov, N.; Jiang, J.; Kaur, S.; Lian, T.; Jackson, L.; Gong, H.; Swayze, R.; Amandoron, E.; Hormozdiari, F.; Dao, P.; Sahinalp, C.; Santos-Filho, O.; Axerio-Cilies, P.; Byler, K.; McMaster, W. R.; Brunham, R. C.; Finlay, B. B.; Reiner, N. E. *J. Proteome Res.* **2011**, *10*(3), 1139.
2. Axerio-Cilies, P.; See, R. H.; Zoraghi, R.; Worral, L.; Lian, T.; Stoynov, N.; Jiang, J.; Kaur, S.; Jackson, L.; Gong, H.; Swayze, R.; Amandoron, E.; Kumar, N. S.; Moreau, A.; Hsing, M.; Strynadka, N. C.; McMaster, W. R.; Finlay, B. B.; Foster, L. J.; Young, R. N.; Reiner, N. E.; Cherkasov, A. *ACS Chem. Biol.* **2012**, *7*(2), 350.
3. Zoraghi, R.; See, R. H.; Axerio-Cilies, P.; Kumar, N. S.; Gong, H.; Moreau, A.; Hsing, M.; Kaur, S.; Swayze, R. D.; Worrall, L.; Amandoron, E.; Lian, T.; Jackson, L.; Jiang,

J.; Thorson, L.; Labriere, C.; Foster, L.; Brunham, R. C.; McMaster, W. R.; Finlay, B. B.; Strynadka, N. C.; Cherkasov, A.; Young, R. N.; Reiner, N. E. *Antimicrob. Agents Chemother.* **2011**, *55*(5), 2042.
4. Zoraghi, R.; Worrall, L.; See, R. H.; Strangman, W.; Popplewell, W. L.; Gong, H.; Samaai, T.; Swayze, R. D.; Kaur, S.; Vuckovic, M.; Finlay, B. B.; Brunham, R. C.; McMaster, W. R.; Davies-Coleman, M. T.; Strynadka, N. C.; Andersen, R. J.; Reiner, N. E. *J. Biol. Chem.* **2011**, *286*(52), 44716.
5. Andrade, M. M.; Barros, M. T. *J. Comb. Chem.* **2010**, *12*(2), 245.
6. Altomare, A.; Cascarano, G.; Giacovazzo, C.; Guagliardi, A. *J. Appl. Crystallogr.* **1993**, *26*, 343.
7. Betteridge, P. W.; Carruthers, J. R.; Cooper, R. I.; Prout, K.; Watkin, D. J. *J. Appl. Crystallogr.* **2003**, *36*, 1487.
8. Farrugia, L. J. *J. Appl. Crystallogr.* **1997**, *30*, 565.